Capstone Final Design Specification

FSAE 1: Electric Motor Gearbox Design

Department of Mechanical and Industrial Engineering

Qilong (Jerry) Cheng 1003834103
Tejvir Binepal 1003750719
Rupin Kothari 1003979545
Syed Nahyan Ahmed 1002616485

Supervisor: Prof. Tony Sinclair

Executive Summary

The University of Toronto Formula Racing Team (UTFR) is a student design team that designs, builds, tests and competes an open-cockpit formula style vehicle in the SAE collegiate series at Michigan and Formula Student competition at Europe each year. The competition consists of static events such as engineering design, business case presentation and dynamic races like acceleration, skid pad and endurance races. The team has done well in the static events and seeks to improve in the dynamic events.

To keep up with competition requirements, UTFR has switched to an electric powertrain with their first electric vehicle in 2022. This has posed problems as the current powertrain is built for a combustion car, and is impractical for an electric motor. Speed reduction is done using a chain and sprocket method at the moment, however, this increases the wheelbase due to the minimum center to center distance required between the sprockets. This issue affects the vehicle handling in tight corners, thus a new electric drivetrain is required.

There were no off the shelf gearbox solutions available for UTFR to use therefore the team has designed a planetary reduction gearbox that is compatible with the motor and the drexler differential. The gearbox provides the required reduction ratio of 4 in the most compact space and connects to the chain and sprocket to allow for adjustability. Lap simulations were done to predict the performance of the design with the car and results show a noticeable improved performance in all dynamic events.

State of the Art gear analysis software KISSsoft was used to iterate through multiple gear designs to determine the optimal planetary gearbox configurations. Gear parameters like the teeth numbers, pressure angle, face width and module were analyzed to result in the best torque to weight ratio. The gears were benchmarked with the ISO standards to ensure adequate safety. In addition, the team ensured all relevant FSAE and Formula Student safety regulations were met. To reduce metal on metal wear, appropriate oil splash lubrication method and associated cooling was determined.

The components of the gearbox were minimized to reduce assembly time and mitigate failure associated with a large number of parts. Excessive weights on each individual parts were also eliminated via the results of the analysis. Structural analysis on the gear, shaft and housing verifies the minimum safety factor to be over 1.3 and structural strength of the design meets the FSAE rules. Vibration analysis was performed to analyze the forced vibration effects. Scenarios like unbalanced rotary vibrations and damaged teeth impact vibrations were considered and their maximum vibration amplitude was estimated. Maintaining the gears are found crucial to minimize the forced vibration amplitude.

Due to the cost constrain, only a 3D printed full scale gearbox was prototyped by the team for the capstone showcase, but with the bearings and screws purchased and assembled with the 3D printed parts. Given the possibility if the client is going to implement the design, the team provided a comprehensive manufacturing plans and assembly plans. Additionally, dyno test plan for performance validation is also included for client's usage. This project aims to expedite the client's transition to an optimal drivetrain architecture and improve performance in dynamic events.

Contents

1 Introduction and Background

The University of Toronto Formula Racing Team (UTFR) is a student-led organization that designs, manufactures, and races a formula-style car in a competition against other universities. The competition consists of static and dynamic event. Static event includes design and business presentations while dynamic event includes acceleration, skid pad, autocross, and endurance races. The static events comprise of 32.5% (325/1000 points) and dynamic events comprises 67.5% (675/1000 points) of the competition points [1]. The team has done well on statics but seeks to gain more points in the dynamics category.

Figure 1: Full Assembly Race Car by UTFR
[1]

In accordance with competition needs, UTFR plans to switch to an electric vehicle (EV) from its current internal combustion vehicle. This change in power source presents a challenge in the design of the vehicle drivetrain which was built for a combustion engine vehicle. Currently, the team is utilizing their previous year's drivetrain system but seeks for a dedicated gearbox for their current EV.
The current drivetrain architecture consists of four main components: the motor and motor output shaft, transmission (chain and sprockets), differential, and driveshafts. Due to the limited space at the rear, the current chain and sprocket method is not practical and results in a wide center to center distance between the motor and differential shaft to ensure sufficient chain wrap. In addition, this minimum center to center distance causes other packaging issues such as a longer wheelbase which affects the turning performance.
The team's chosen Slovenian motor, EMRAX 228, is not based on National Electrical Manufacturers Associations (NEMA) standards [2] which is why there is no readily available off-the-shelf gearbox for usage. Therefore the main problem our team will tackle is to design a compact reduction gearbox that is compatible with the EMRAX 228 motor and the Drexler differential. As such the team is required to:

- Integrate the proposed design with the current motor and differential.
- Design components that are not readily available for the team.
- Research and develop a testing and bench marking method for the proposed system.

Successful execution of the new design will provide UTFR with a readily tested and manufactured gearbox that can be used directly with the motor. Furthermore, it will reduce the time frame for the team to implement the system for upcoming competitions.

[1] Car Image Courtesy of UTFR

1.1 Scope

The scope of the project will include the mechanical design of the gearbox, which will connect the motor to the differential. Designing the differential is out of the scope since the team will utilize the existing FSAE Drexler model. The scope also includes a selection of electronic sensor hardware that will measure the critical parameters of the gearbox, namely the output speed and temperature of the lubricant inside the gearbox. The wiring of the sensors is also outside the scope of the project.

The design will include the structural housing for the gears, shaft layout, and gear reduction stages. LapSim analysis will be done to determine the optimized gear ratio for the car. Structural analysis on the components will be performed to ensure that the gearbox will be stable under desired loading conditions. Under certain conditions, the gear operation might generate heat, which could break down the lubricant layer. To account for these factors, suitable cooling techniques will be developed.

The goal of this project is to develop a prototype of the gearbox that can be bench tested with the EMRAX 228 motor to demonstrate functionality. The test will demonstrate if the output torque and speed are proportionately modified as per the design intent.

To aid in testing manufacturing within budget, suitable modifications will be made as the design is not intended to go on the team's 2022 competition vehicle. Based on the testing results and any required modifications, complete mechanical drawings and CAD models will be provided for a unit that UTFR can utilize to build the customised gearbox.

Besides the 500 dollars budget, UTFR will fabricate materials and provide access to the manufacturing facilities. For big-budget items, the team will approach the client to purchase components that they think are valuable.

2 Project Requirements

2.1 Functions

To summarize, the designed gearbox must perform the following functions to solve the problem identified in Section 1.2

Table 1: Functions of the Design

Function No.	**Function**
Function 1	The design must be able to transmit motion and energy from the motor to the differential
Function 2	The design must be able to increase the torque to the desired output

2.2 Objectives

Table 2: Design Objectives and Justification

Weight	Objective	Metric	Justification
10	Mass	$\leq$ 20 kg	Better acceleration is associated with lower mass
10	Volume Footprint	$\leq$ 406.4 mm $\times$ 190.5 mm $\times$ 127 mm	Space constraint in chassis provided by client
9	Cost	$\leq$ 1000 CAD	Must be within the budget provided by UTFR
8	Assembly Time	$\leq$ 2 hours	In the event of replace/repair of component, UTFR will have adequate time during events
7	Moment of Inertia	$\leq$ 0.028 kg.m^2	Benchmarking with current UTFR vehicle. Design should output better performance .
6	Gear Ratio	3 - 5	Best output in terms of speed and torque balance from the motor as per Figure 69.
5	Efficiency (Output Power)	$\geq$ 90%	Design should minimise efficiency loss
4	Service Life	$\geq$ 350 hrs	Gearbox needs to be operational during the testing and competition phases (for 1 season)
3	Safety Factor	1.2	To account for raw material's quality and manufacturing defects
2	Operating Temperature	$-29°C$ to $57°C$	Design must be operable in a range of environments depending on the event's location

2.3 Constraints

Every candidate design must fulfill these requirements. These are based on resources available for the project, safety, and compliance with competition rules so that the design can be used for racing.

Table 3: Design Objectives and Justification

Constraints	**Descriptions**
Manufacturability	Must be manufacturable through UTFR's resources
Compatibility	All mounts and connections must be compatible with the team's steel tube chassis.
Fasteners	All fasteners must follow critical fasteners guidelines as per FSAE rules T.8.2 [1]
Shield	All exposed powertrain rotating parts must be covered with a scatter shield to contain them in case of failure T.5.2 [1]
Electrical Safety	Any housing/casing containing parts electrically connected to the high voltage tractive system must display ISO7010-W012 stickers as per FSAE rules E.V 5.9 [1]
Grounding and Flash Protection	Any parts near a high voltage tractive system must have a resistance that meets specifications listed in FSAE rules E.V 7.7 [1]

2.4 Stakeholder Analysis

Table 4: Stakeholder Analysis

Stakeholders	**Descriptions**
Faculty and Students	The Capstone Office at the University of Toronto have provided our team with a substantial amount of money and access to the machine shop to design, develop and test the final design prototype, which will eventually be used in the 2023 UTFR vehicle. In addition to the above-mentioned, winning the competition will be a success for UofT on the global stage. This can be translated into more funding for the UTFR team in the future.
UTFR's Sponsors	Moving to electric vehicles could lead to companies, which are currently investing in EV technology and electric chargers to invest in the club's projects. This would also drift away companies that are currently supplying combustion engines and other components, which won't be used anymore in future projects.
UTFR club	A successful integration of the gearbox into the new EV will lead to gaining more competition points and improve global standing.The UTFR team is solely responsible for the manufacturing and servicing of their EV. The new gearbox designed for the EMRAX 228 motor will be extensively tested by their team for reliability and safety purposes. New safety and maintenance procedures might be developed for the proposed design to account for all the changes. This will ensure smooth integration with existing components (Electric motor and Differential).
Driver	The driver will be the primary user of the end product, hence the design must meet safety requirements as per the FSAE rules.
FSAE organizers	The organizers are concerned with the safety of the drive train system, which is going to be incorporated in the 2023 EV. Extensive safety and reliability inspections will be performed on the EV vehicle before it can take part in the competition, in order to make sure all the regulations are met and satisfied.

2.5 State of the Art Review

The state of the art review provides us with insights and comparisons with current solutions. Due to the unique service environment, all gearboxes for the EMRAX 228 motor are custom designed. Those existing gearboxes gave us a better understanding of the design principles utilized while manufacturing them and assisted us to benchmark our candidate designs. Two noticeable examples are shown below from the Highlander Racing team and Melbourne University Racing Team.

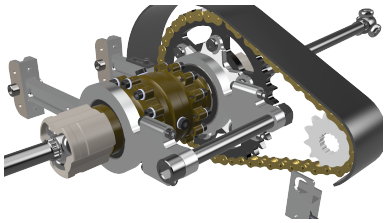

Figure 2: Melbourne University Racing Team Electric Drive Train Design

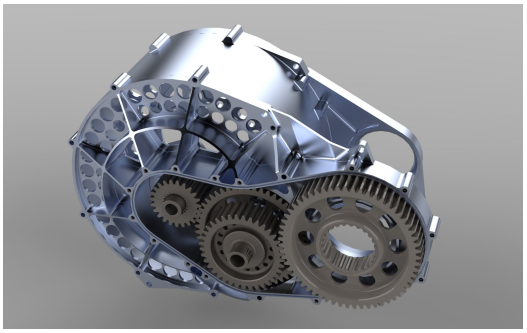

Figure 3: Highlander Racing Team Gearbox Housing and Gears Placement

Table 5: State of the Art Summary

Teams	**Gear Ratio**	**Motor**
UC Riverside Highlander Racing Team	Not available	EMRAX 228 [3]
Wisconsin Racing	4.5:1 [4]	Nova 30
Illinois Formula Electric	3.58:1 [5]	EMRAX 228 [5]
Penn Electric Racing	10:1 [6]	EMRAX 228 [6]

2.6 Service Environment

The design will be utilised in numerous operational environments. Therefore, the design must be functional for the listed environments:

Table 6: Types of Service Environments and Their Condition Descriptions

Service Environments	Descriptions
Manufacturing	Parts will be manufactured at the University of Toronto's machine shop and then will be assembled at UTFR's workshop. Dust and debris can be encountered during the assembly process.
Transportation	A trailer will be used for transporting UTFR's vehicle to testing venues and the Michigan international speedway for competition. The average monthly temperatures and precipitation from March to October are listed in Appendix B, which is when the transportation will be taking place. Additionally, a wooden crate, is used for shipping the EV to Germany. Overseas transport normally takes around one month by vessels, and the temperature changes dramatically from as low as -29 °C to as high as 57 °C.
Operational	1. Track Testing Operational Service Environment: Track testing will occur between March to October. Most of the track testing occurs on asphalt with negligible debris. The test tracks will be at the GO parking lot (a lot of debris), Gamebridge Go-Karts (negligible debris, rubber from go-kart wheels), Flamboro Speedway, and miscellaneous parking lots. 2. Competition Operational Service Environment: The average temperature and precipitation during the competition are listed in Appendix B. The competition tracks include Autodrom Most (Czech), Michigan International Speedway (Michigan), Hockenheim (Germany), and Las Vegas motor speedway (FSAE Nevada) which are pristine and have no debris.

2.7 Design for X

To achieve the targeted performance in specific objectives, the Design for "X" methodology is used where X is replaced by the area of focus. Manufacturability, serviceability, and reliability were determined to be the key aspects. The following guidelines will be followed to achieve these goals

2.7.1 Reliability:

In order to achieve success, the design must be able to perform as intended during the testing and competition phase. In order to ensure system-level reliability, a simpler design with fewer components would be preferred over a high-performance design with multiple components. To ensure structural reliability, safety factors will be incorporated after load case analysis of specific components.

2.7.2 Manufacturability:

UTFR relies extensively on students to machine the majority of the drive-train components and only a few important processes like splining, gun drilling, etc. will be outsourced. Off-the-shelf components like gears, shafts, and bearings can be bought from a third-party supplier since that would be more cost-effective.

2.7.3 Serviceability

Off-the-shelf components will be used wherever possible to develop the gearbox in order to allow for easy swapping in case of failure. For custom design parts, the machining and assembly time will be taken into account so suitable replacements can be made within the limited time frame.

2.7.4 Cost

UTFR has a limited section budget for power train components since majority of the cost is incurred in purchasing the electrical components such as battery modules (fixed cost). Hence the proposed design should minimise cost.

2.7.5 Safety

The gearbox is a critical component of the vehicle, and any failures should be prevented regular operation. Because the driver will be in close proximity to the gearbox, safety for the driver is part of the design consideration. Due to the high torque and rotational forces within the components of the design, the components and packaging needs to be made with a minimum level of safety.

3 Concept Generation

Given the project requirement and objectives stated above, various designs ideas are generated to solve client's problem. Mainly, Brainstorming and Morphological Chart were used to determine the possible candidate solutions. In total three candidate designs that fits the objectives were investigated in details, as shown in Figure 4.

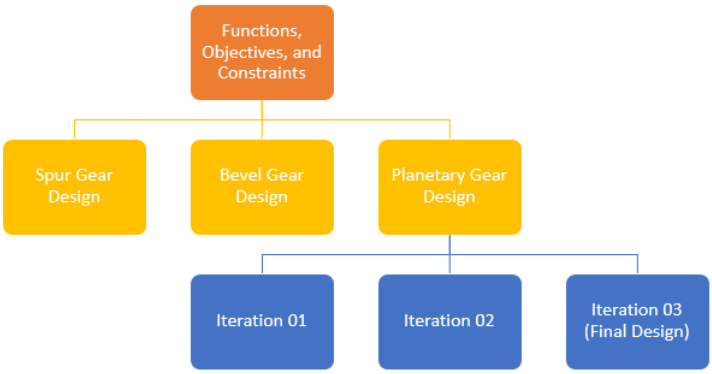

Figure 4: Candidate Design Adoption Process

3.1 Candidate Designs

3.1.1 Bevel Gearbox

The Bevel Gearbox consisted two sets of a 40-20 tooth gear pair meshed at 90 degree angle. Notable aspect of this design was the fact that the motor and differential were beside each other giving us a compact design. However, the flank safety of 1.015 and root safety of 1.4 is too low considering the application of the design.

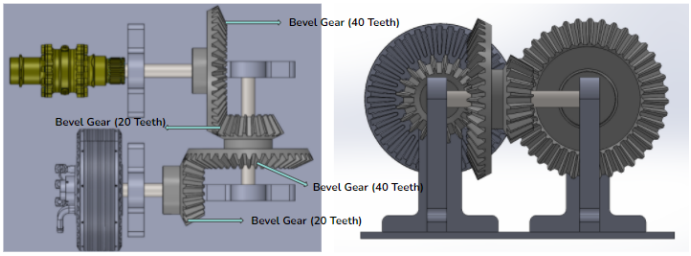

Figure 5: Bevel Gearbox Design

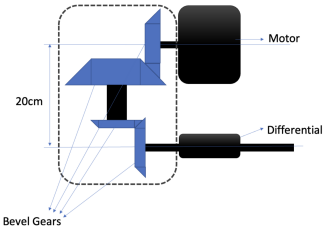

Figure 6: Bevel Gearbox Mechanical Schematics

3.1.2 Spur Gearbox:

The Spur Gear design consisted a set of 30-60 and 40-80 tooth gear pair meshed and interconnected to each other. The gear shafts are parallel to each other. However, achieving an ideal gear ratio will exceed the size constraint within the chassis therefore, another design needs to be considered.

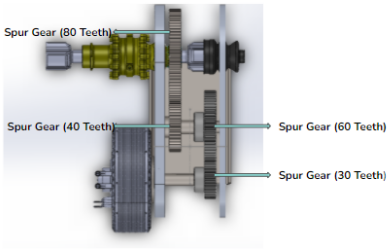

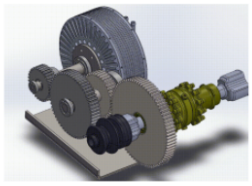

Figure 7: Spur Gearbox Design

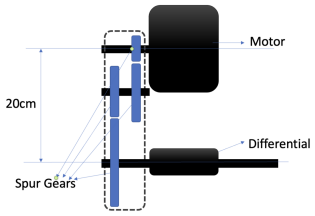

Figure 8: Spur Gearbox Mechanical Schematics

3.1.3 Planetary Gearbox:

The Planetary Gearbox Design is more compact and is able to output a high gear ratio. It features a set of four planet gears around a sun gear that is connected to the input shaft of the motor. The output shaft, also known as the output carrier, connects to a chain and sprocket system. The ring gear is held stationary by the two housings in between and grounded onto the chassis of the vehicle. Overall, the power flows from the motor, to the input shaft which is directly connected to the sun gear. Then the sun gear transmits it to the surrounding four planet gears. Since each planet gear is held by the planet shaft , the energy passes to the output carrier and onto the chain and sprocket. Finally, chain and sprocket transmits the motion to the differential of the vehicle. The schematic of the planetary gearbox is shown below:

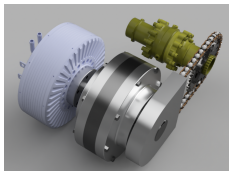

Figure 9: Render for Planetary Gearbox Design

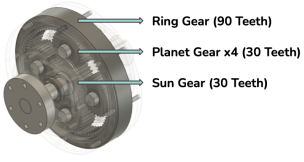

Figure 10: Planetary Gearbox Design

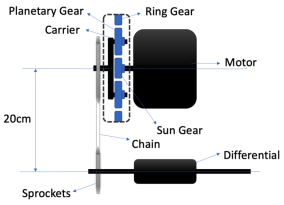

Figure 11: Planetary Gearbox Mechanism Schematics

Final Design Selection: The Planetary Gearbox Design is selected for its ability to output a high

gear ratio in a compact space compared to the bevel and spur gearbox design. Being compact also translates to a relatively lower mass and cost compared to other two candidate designs. A weighted decision matrix used to compare the three designs is provided in Appendix C.

3.2 Design Iteration

Figure 12 shows the iterative process, used to improve the planetary gearbox design. The team started with an initial design that met functionalities and critical objectives, and then iterated each components' designs to meet the other objectives. To get our final design, it went through three most noticeable iterations which are listed below.

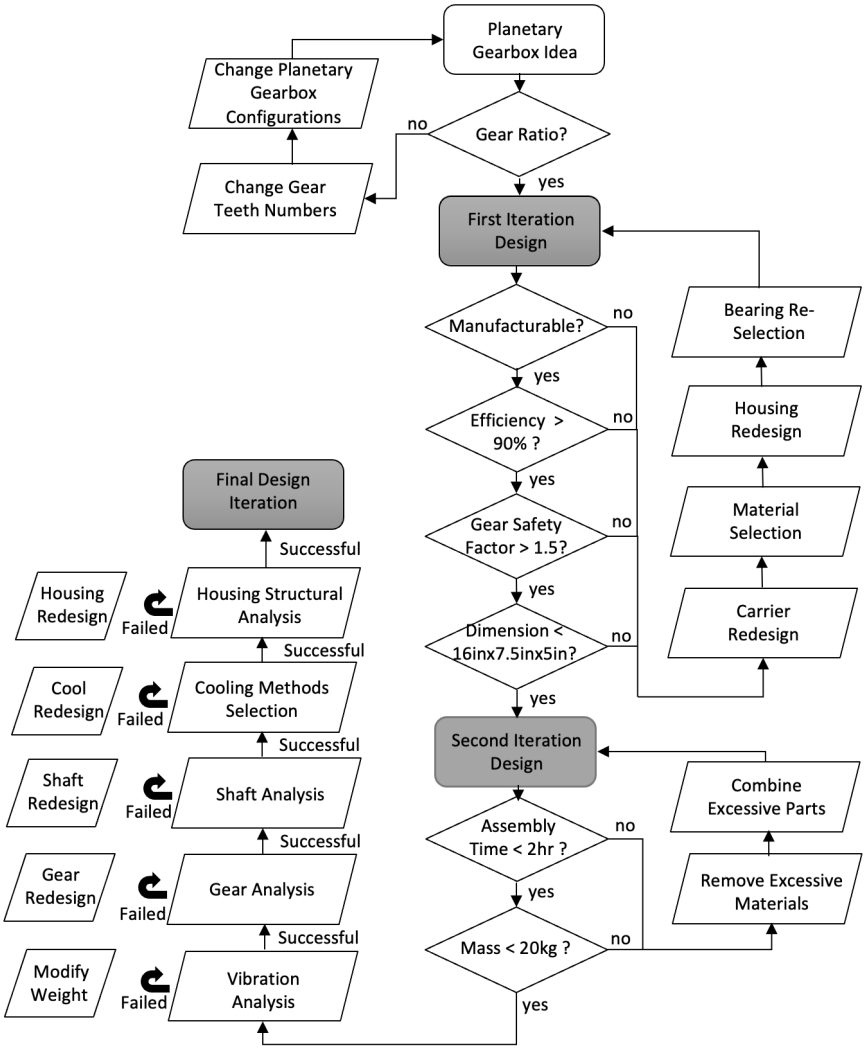

Figure 12: Design Iteration Flow Diagram

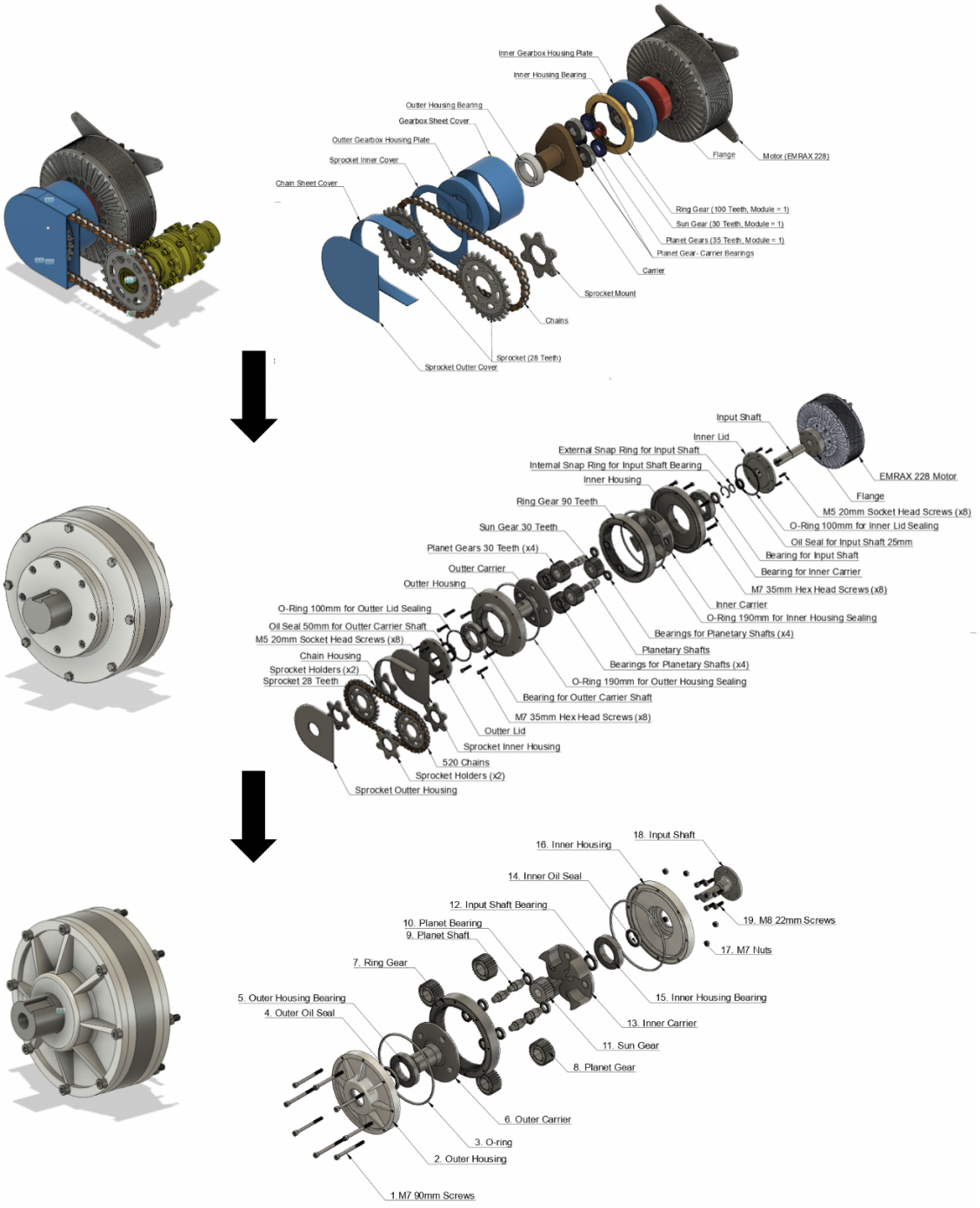

Figure 13: Three Iteration Design Overview

Table 7: First Design Iteration Changes and Decisions Descriptions

Part Illustrations	Descriptions
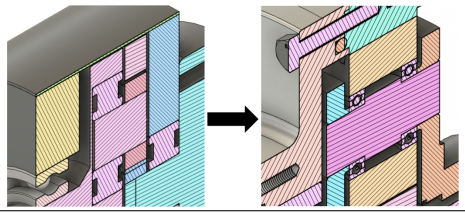	**Added Bearing Spacer Integration:** Spacer are added to prevent generated friction when the rotational part of the bearings are in contact with the stationary parts. Instead of using off-the-shelf bearing spacer components, spacers are directly integrated with the components themselves to eliminate the assembly difficulty.
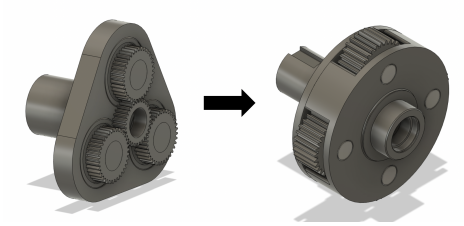	**Doubled Carrier** Compared to the single carrier design, doubled carriers fix the planet pins on both ends, reducing the bending stress by providing more supports. **Four Planets** By increasing the number of planet gears from three to four, it decreases the stress on each planet gear teeth, and increases the overall safety factor. (Simulation on KissSoft can be referred to Appendix G). In addition,
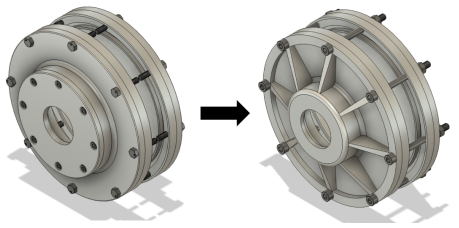	**Simplified Housing Design:** A uniform two-piece aluminum housing design is chosen to replace the previous four piece housing design. This reduction simplified the assembly process and reduced the cost in terms of total number of M8 screw required. In addition, a one piece aluminum housing design is able to reduce the total volume and mass by eliminating the connector area (where screws thread in). Finally, to achieve the same structure rigidity, new webs are implemented to ensure housing's strength. This not only reduces the total weight by 3.2kg but also increased the surface area for better air convection cooling.
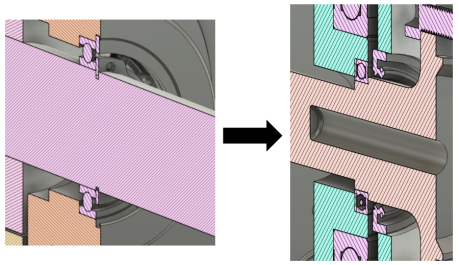	**Simplified Bearing Fitting Method:** Unlike the previous iteration which used snap rings and deep grooves on the shaft, the bearings are retained using shaft shoulders. In this iteration all bearings are press fit into the components. To separate the inner and outer part of the bearing with the moving piece, integrated spacer are designed onto the components to eliminate additional pieces.
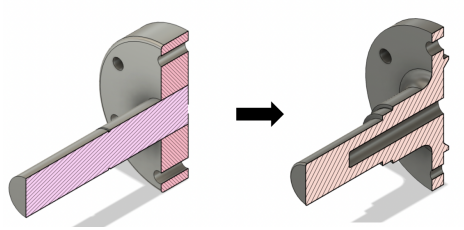	**Modified Motor Flange:** Compared to the two separate pieces for motor flange and the input shaft, the updated iteration combined the two piece into one as shown on the left. Because the previous input shaft is press-fit into the motor flange, this can cause safety issues too when the manufacturing tolerance is outside what the press fit dimension is desired. By combining them into one piece avoids this safety hazards and also reduced the weight by

4 Final Design

A 4:1 gear-ratio customized planetary gearbox and a chain and sprocket system were designed to be compatible with the EMRAX 228 motor and Drexler differential. The design focused on being lightweight, compact, and easy to assemble. First, the motor outputs the power to the planetary gearbox before connecting to a chain and sprocket for offsetting the rotational movements to the differential. This design allows to have a four-times torque output while allowing the flexibility to modify the total gear ratio by changing the size of the sprockets easily. The final design decreased the overall mass by nearly 5kg compared to the initial designs and reduced over ten excessive parts. After all the iterative deign processes, the final gearbox is rendered as shown below:

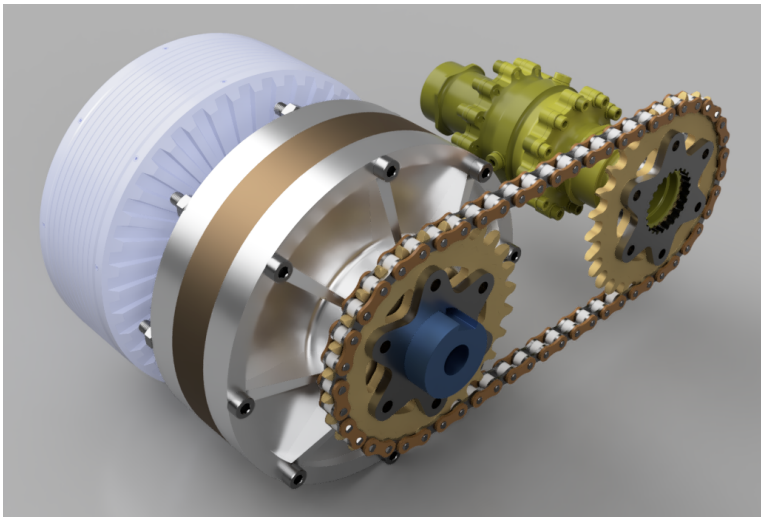

Figure 14: Final Design

4.1 Planetary Gearbox Specifications

All the Final Design Specifications are summarised in Appendix D.

Table 8: Design Objectives and Final Design Specifications

Parameters	**Target Values**	**Final Design Specs**
Mass	$\leq$ 20 kg	15.4kg
Volume Footprint	$\leq$127mm*190.5mm*419.1mm	126.6mm*224mm* 224mm
Cost	$\leq$ 1000 CAD	5000 CAD
Assembly Time	$\leq$ 2 hours	1 hour
Gear Ratio	3 - 5	4 (4.0 for planetary; for chains and sprockets – changeable based on client's needs
Service Life	$\geq$ 350 hrs	1000 hrs
Safety Factor	1.2	Root safety 2.5, Flank safety 1.4
Operating Temperature	-29-57 °C	-23.3-40 °C [7]

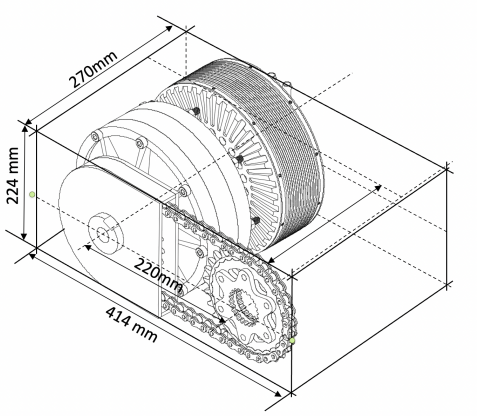

Figure 15: Final Design and Its Overall Dimension

4.2 Material Selections

Strength to weight ratio of various materials was compared using an Ashby Plot as shown in Figure 16. For the Shafts and Housing, material from top right of the graphs were chosen to be the best candidate.

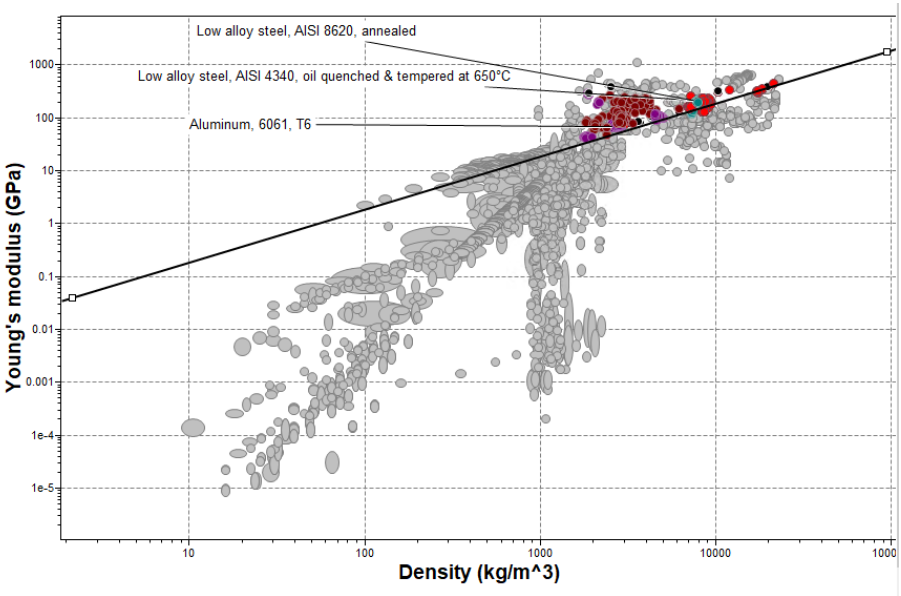

Figure 16: Materials selected for Shaft, Gears, Carriers, and Housing

Non-metal materials have been filtered out from the material selection process. This is because of the service temperature that the design will be operating in. Specialized composite materials such as Carbon and Aramid Polymer fibers have also been filtered out due to their high costs.

- **Housing – Aluminum 6061-T6:**

  The material for housing is chosen as a cheaper metal. It also has to be a heat conductor so that the cooling method can transmit the heat produced within the design away. It has excellent corrosion resistance and superior machinability and weldability.

- **Shafts and Carriers – AISI 4340:** Shafts, and Carriers are the critical components of the design. AISI 4340 alloy steel is a heat treatable and low alloy steel containing chromium, nickel and molybdenum. It has high yield strength and is widely used for manufacturing shafts.
- **Gears – SAE 8620 steel:** Gears are often heat treated post machining for added strength. Both alloy steels (SAE 8620, 5120) and through hardening steels (1045) were considered. SAE 8620 steel was chosen due to it's wider availability and lower cost.

4.3 Component Selections

The component selection was done intuitively. The gears were chosen first to determine the overall dimensions and placement. The bearings were chosen next based on the choice of gears and the intended service life. Once the overall layout of the gearbox was determined, the remaining components such as fasteners, O-rings and seals and lubricants were determined. Finally the chain was chosen to transmit the modified torque.

4.3.1 Gear Type

The objective of the gear selection was to ensure high speed and high torque handling capability while minimizing the cost. Straight Spur Gears, Helical Spur Gears and Herringbone gears were compared. Table 8 shows the comparison between the gear types. Straight spur gears were chosen due to their ability to best meet these objectives while minimizing the cost.

Figure 17, Figure 18, Figure 19 below illustrate the different gear types considered

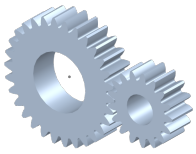

Figure 17: Straight Spur Gear [8]

Figure 18: Herringbone [9]

Figure 19: Helical Spur Gear [10]

Table 9: Types of Gears

Gear Type	Shaft Alignment	Torque	Speed	Contact Ratio	Noise	Tribology	Cost
Straight Spur	Parallel	Low to High	High	1.3-1.8	High	Good	$
Helical Spur	Parallel	Medium to High	Medium to High	2-3	Low	Okay	$$
Herringbone	Parallel	High	High	2.5-3	Low	Okay	$$$

4.3.2 Gear Parameters

Gearbox Configurations: (z_a is the number of teeth for sun gear; z_b is the number of teeth for planet gear; z_c is the number of teeth for ring gear) The planetary gearbox presents an opportunity to provide various modes of operation depending on the constraint gear-pair in the system. These configurations and the choice used for the design are described below:

- **Free Rotation Type:**

  In this configuration the input is the sun gear and the output is the carrier, however, the ring gear is not held stationary. This will give a 1:1 ratio [39]

$$r_{free_rotation_type} = 1 \tag{1}$$

- **Planetary Type:**

  Input: Sun gear; Output: Carrier; Ring gear is held stationary
  Gear ratio can be found using equation: [11]

$$r_{planetary_type} = \frac{z_c}{z_a} + 1 \tag{2}$$

- **Solar Type:**

  Input: Ring gear; Output: Carrier; Sun gear is held stationary
  Gear ratio can be found using equation: [11]

$$r_{solar_type} = \frac{z_a}{z_c} + 1 \tag{3}$$

- **Star Type:**

  Input: Sun gear; Output: Ring; Carrier is held stationary
  Gear ratio can be found using equation: [11]

$$r_{star_type} = -\frac{z_c}{z_a} \tag{4}$$

Since a high gear ratio is required, the Planetary Type is chosen as our design for its highest gear ratio output amount the four different configurations.

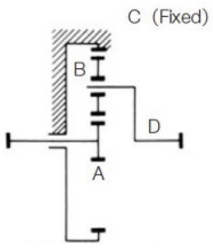

Figure 20: Planetary Type Illustration [11]

Pressure Angle: Pressure angle is the angle between tangential of the two contact surfaces for the gear teeth and its radial line. The most common off-the-shelf gears have pressure angles of 14.5° and 20° as shown in the figure below.

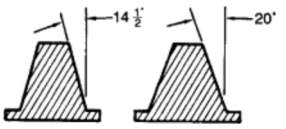

Figure 21: Pressure Illustration

In our design, 20° pressure angle is chosen because it results in a higher strength gear tooth that offers better wear-resistance characteristics. The use of a 20° angle also permits pinions with fewer teeth to be used[12][13].

Gear Teeth Number: The relationship between number of teeth for the planet, sun and ring gear follows the equation below:

$$z_c = z_a + 2z_b \tag{5}$$

Another important consideration was determining the minimum number of gear teeth on the pinion to avoid interference with the gear [14]. Once the number of teeth on the pinion is determined, the planet gear teeth number to avoid interference can be determined using the equation given below.

$$T1 \geq \frac{2a_w \frac{1}{T_2} P_d}{\sqrt{1 + \frac{1}{T_2}(\frac{1}{T_2} + 2)sin^2\phi} - 1} \tag{6}$$

In combination with the above gear ratio calculation, a few gear teeth numbers were chosen as candidates. Moreover, selected gears are selected based on standard off-the-shelf gear teeth numbers that can be easily acquired.

Table 10: Gear Teeth Number Combination Candidates

Ring Gear	**Sun Gear**	**Planet Gear**
90	30	30
100	30	35
120	40	40
120	30	45

The 90 teeth ring gear combination is chosen for its smaller footprint. For a pressure angle of 20 the minimum number of teeth on the pinion is 13. The choice of a 30T-30T gear pair is well over this number. On determining the number of teeth, the contact ratio between the sun-planet mesh was calculated to be 1.8 and 1.805 for the planet - internal gear mesh. This exceeded the threshold ratio of 1.2 used for good practice.[12]

Module: Modules 1 to 4 were compared to determine the best module for maximizing the torque to weight ratio. In general, a higher module means a larger sized gear. It was determined that module 2mm with a pressure angle 20 provided the best optimal compromise between size and weight and hence was chosen for the design.

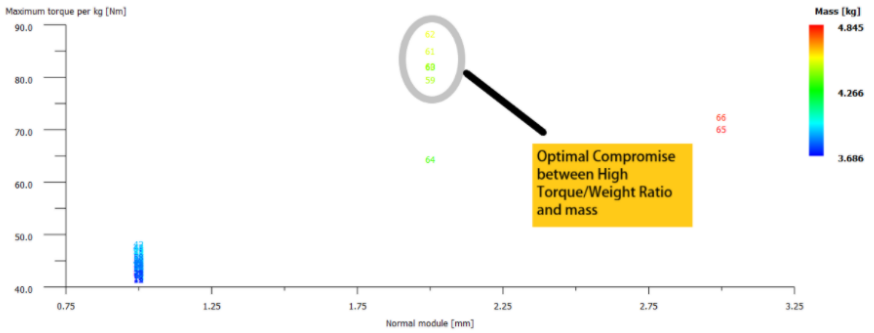

Figure 22: Module Comparison

In the final design the geometric parameters of each gear is listed below:

Table 11: Geometric Parameters of Gears in the Planetary Gearbox

	Tooth Number	**Module(mm)**	**Pressure Angle (°)**	**Gear Face Width(mm)**
Sun Gear	30	2	20	30
Planet Gear	30	2	20	30
Ring Gear	90	2	20	30

4.3.3 Bearings

The choice for gears determines what kind of bearings are needed. Since the gears used are straight spur gears, no axial force is subjected on the shaft. Therefore the need for cylindrical roller bearings can be eliminated. Deep groove ball bearings are low cost and able to withstand large loading conditions in high speed. This fits our design objectives to be low cost, safe and provide high torque at high speed. Finally, since the application would encounter a lot of dirt and debris, sealed deep groove bearings are chosen as our bearing selections.

Table 12: Bearing Selection Summary

Part	**Dimensions (ID-OD-width)**	**Bearing Trade Number**
Ball bearings for planetary gears - planetary shafts	20mm-32mm-7mm	6804-2Z
Ball bearings for carrier and housing	55mm-100mm-21mm	6211-2Z
Ball bearing for input shaft and carrier	25mm-37mm-7mm	6805-2Z

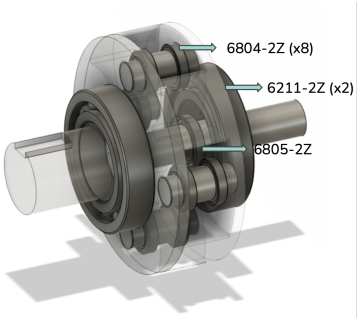

Figure 23: Selected Bearings and Their Placement

4.3.4 Lubrication

Gearboxes rely on lubrication to reduce friction for optimal operation and life [15]. The gearbox operates in both high speed and high torque application. A lubricant with a viscosity that is too high for the application won't flow sufficiently as the gear teeth engage to protect mating surfaces and provide cooling. On the other hand, low viscosity won't provide a sufficient film thickness to prevent metal-to-metal contact. Due to the high speed requirements it is preferred to have a lubricant that is not highly viscous yet can prevent from breakdown during high operational temperature.

There are three methods of lubrication commonly used in a gearbox:

- Grease Lubrication
- Oil Splash Lubrication
- Forced Oil Lubrication

The use of those lubrication methods is determined based on the gear's tangential speed, and it can be referred to the table below:

No.	Lubrication	Range of tangential speed v (m/s) 0 5 10 15 20 25
1	Grease lubrication	←→
2	Splash lubrication	←→
3	Forced oil circultion lubrication	←

Figure 24: Lubrication Selection Reference [15]

The speed of the gears in our design is calculated to be 8m/s (Detailed Analysis can be found in Section 5.5), which falls in the range of Oil Splashing Lubrication method. As a result, oil over grease is used in the design

4.3.5 Screws and Nuts

The design of the fasteners is a safety constraint of the project. The FSAE rules classify all powertrain fasteners as critical fasteners. These fasteners must be GRADE 8.8 or stronger, and they must have a positive retaining mechanism such as a cotter pin/nylon lock nut and two threads sticking after fastening as per rule T8.1 [1]. In the competition rules M8 bolts are recommended to meet this requirement. The screws were designed to be fitting through all two housing pieces and the ring gear in place, and 22cm screw length is chosen so that it leaves follows the FSAE rules.

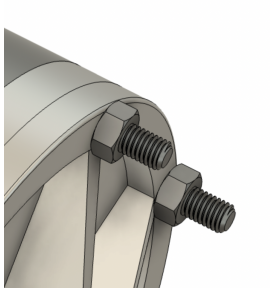

Figure 25: Screw and Nuts Clearance Illustration

Finally, as the housing will be subjected to a maximum stress of 9.2MPa (Referred to Section 5.4), partially threaded bolts are chosen over the fully threaded ones. Partially threaded screws are better for resistance and alignment, which helps the tight seals of the gearbox as well. The non-threaded segment, known as grip length, contains zero weak spots to prevent strain at this peak stress point [16].

Figure 26: Partially Threaded Bolts

4.3.6 Sealing (O-rings and Oil Seals)

To ensure good sealing and prevent lubrication from leaking during the race, O-rings and Oil seals are used inside the gearbox to create an air tight environment. The O-ring is mainly used between Housings and Ring Gear's contacting surfaces, while the Oil Seal is used to seal the rotating shafts.

- O-rings:

  The O-rings are selected based on McMaster Carr website as standard off-the-shelf parts. The Ring Gear has an inner diameter of 180cm and an outer diameter of 220cm, the O-rings are selected to be with 190cm inner diameter and a 5mm of width. This also makes clearance for the threaded screws to go through the ring gear. The 4mm groove indent is made based on the 5mm width dimension of the O-rings themselves.

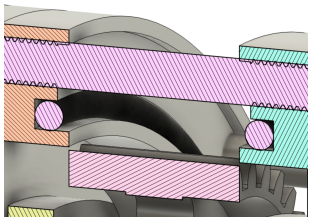

Figure 27: O-rings inside the Housing Deep Grooves

- Oil Seals:

  Similar to the O-rings, Oil Seals are also selected from the off-the-shelf components on Mcmaster Carr. The inner diameter of the oil seals have the same diameter as the input and output shafts.

To summarize, the selected oil seals and o-rings are listed in the table below:

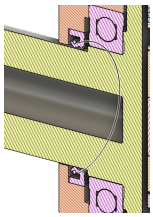

Figure 28: Oil Seal at the Output Shaft

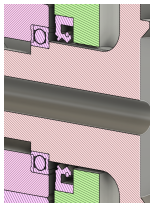

Figure 29: Oil Seal at the Inner Shaft

Table 13: Oil Seal

Part	**Dimensions (ID-OD-Width)**	**Identification Number**
Oil seal for input shaft	25mm-35mm-7.3mm	1199N14
Oil seal for output shaft	50mm-65mm-8.3mm	1199N327
O-ring for housing	190mm-200mm-5mm	1302N267

4.3.7 Chains and Sprockets

Rotational motion transfer from the motor to the differential can be done by either belts & pulleies or chains & sprockets. Belts have issues related to slippage and wear which is detrimental to their long term use. On the contrary, chains and sprockets are able to provide more strength with less slippage. Moreover, the differential used by UTFR currently is rated for the chains and sprockets. Therefore, the team concluded that chains and sprockets is best suited for motion transfer. The 520 motorcycle chain is chosen for our design because of its strength and weight balance, also it is already current available for the UTFR team and has been used in the past contests.

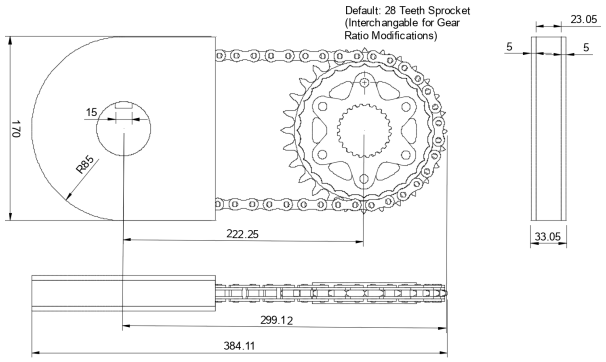

Figure 30: Chain and Sprocket Dimensions

Table 14: Chain And Sprocket Specifications Summary

Chain Type	**Size**	**Force (kN)**	**Weight (kg/100 links)**	**Length (m/100 links)**	**Weight per length (kg/m)**	**Force /Weight (kN/kg)**	**Total Mass (kg)**
Super O-Ring NZ	420	21.9	0.82	1.27	0.65	33.9	0.420
O-Ring	428	25.5	1	1.27	0.79	32.4	0.512
O-Ring	520	35.8	1.61	1.59	1.01	35.3	0.659
O-Ring	525	39.2	1.81	1.59	1.14	34.4	0.741

A 18:20 ratio is selected for the chain and sprocket to enable UTFR to use their current design without modification. The minimum number of teeth is chosen as 18 to avoid insufficient chain wrap. This ratio can be adjusted based on track configuration to achieve further performance enhancement. Using chains and sprockets also allows the differential to be placed at the same distance away from the motor as the current race car configuration. Additional chain guards will prevent debris from getting into the chain. Routine maintenance of the chain before events will enable optimal performance of the chain and sprocket.

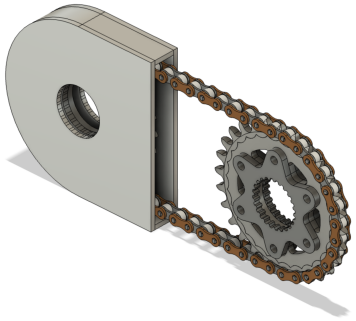

Figure 31: Chain and Sprocket Overview

Table 15: Chain And Sprocket Dimensional Specifications for 520 Motorcycle Chains

Parameters	**Numbers**
Chain Size	520
Pitch	0.625”
Roller Width	0.250”
Roller Diameter	0.400”

5 Analysis and Validations

5.1 Simulated Performance Analysis

Optimum Lap was used to simulate the vehicle performance with the updated final drive ratio of 4.0 compared to the previous final drive ratio of 3.0 [17]. Since the motor is not able to sustain Peak

Torque over a longer period of time, the motor's Continuous Torque Curve (green) was utilised for simulation as per Figure 32.

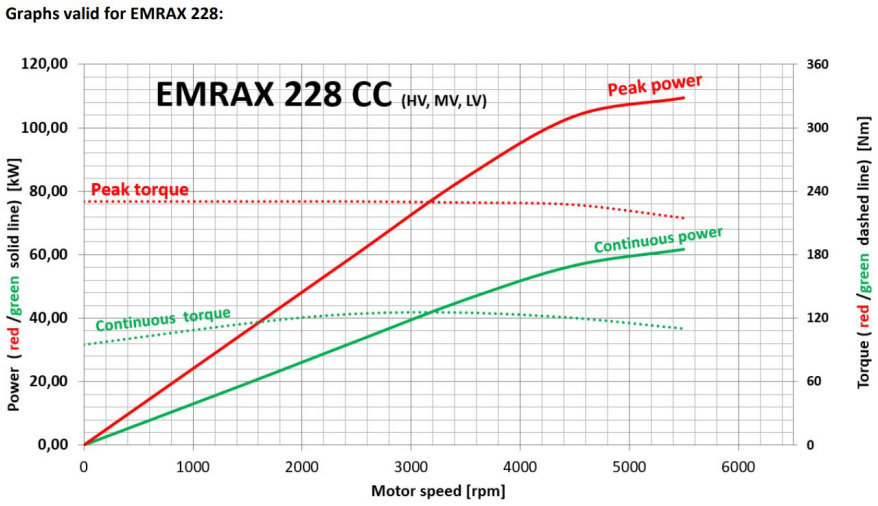

Figure 32: Motor Dyno Curve [18]

The most noticeable change in lap time is during the endurance where the new design saves a total of 3 seconds. Figure 33 shows a track map comparing the current final drive ratio of 3.0 with the proposed ratio of 4.0. Because the simulation is a one-dimensional model, the treads rather than numerical values were used for qualitatively comparison. It can be seen that the proposed design achieves a higher top speed in straight sections.

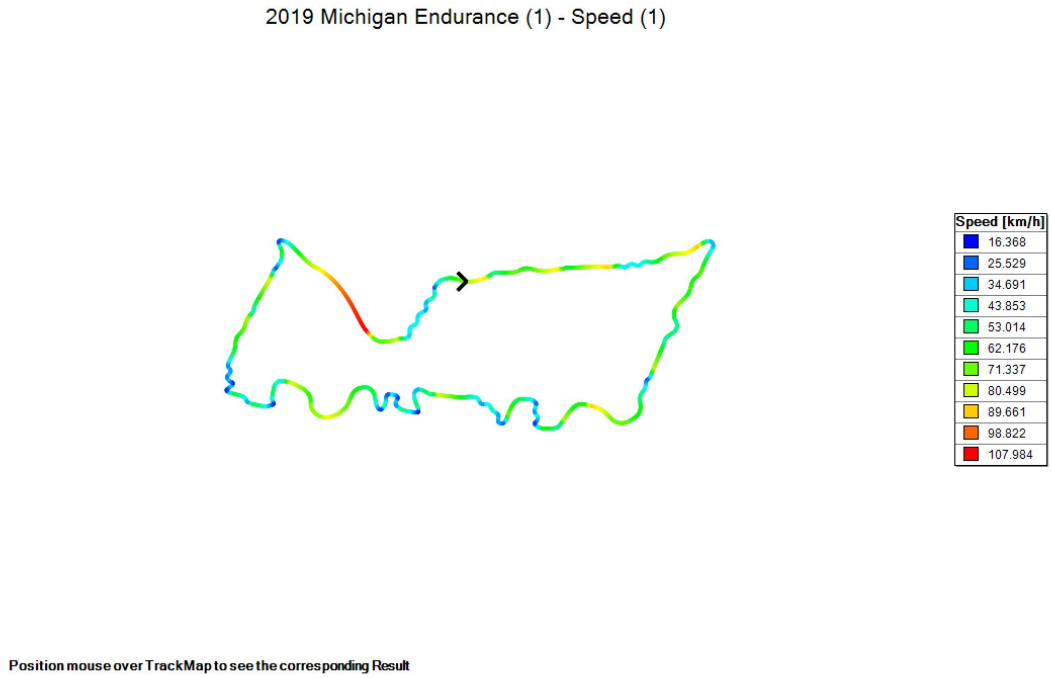

Figure 33: Track Map Simulation with a ratio of 3.0

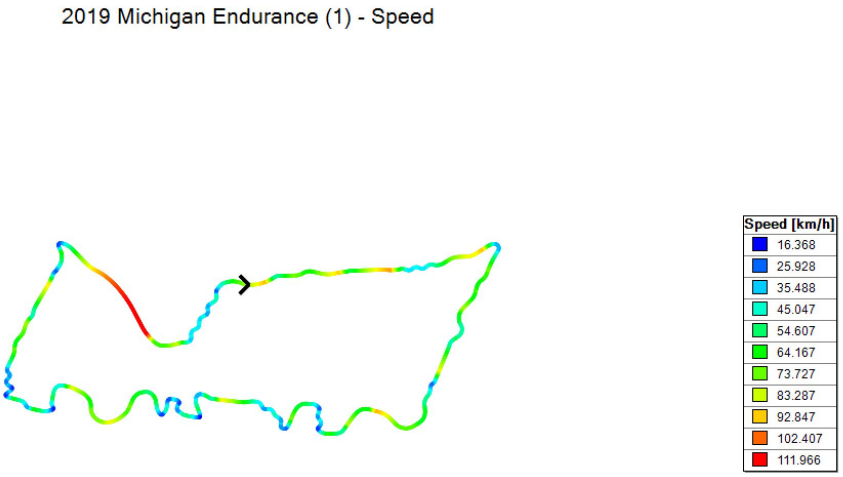

Figure 34: Track Map Simulation with a ratio of 4.0

More tractive force can be generated with a higher gear ratio which allows for more acceleration out of the corner to reach a higher top speed. Figure 35 shows that the new gear ratio provides adequate tractive force in the operating speed range of 20km/hr-65 km/hr, which is the average operating speed during competition races.[1]

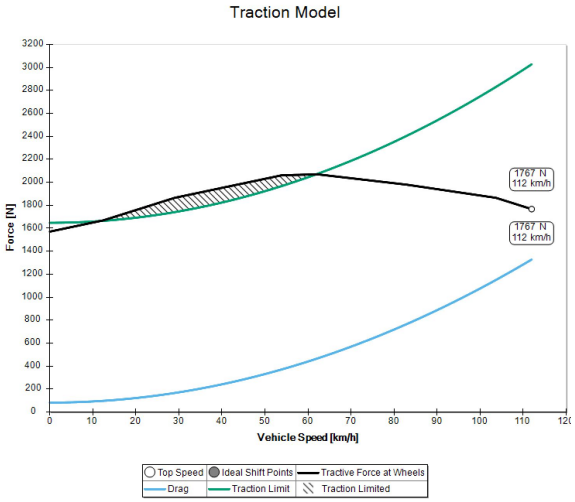

Figure 35: Gear ratio of 4.0

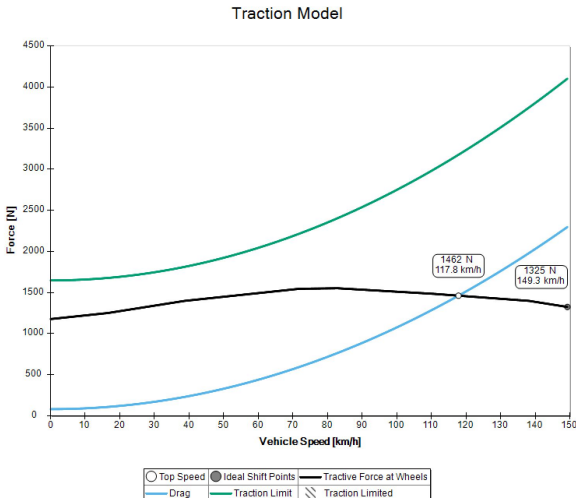

Figure 36: Gear ratio of 3.0

Table 16: Performance Simulation Using Lap Simulation

Race	**UT 21 EV**	**New Design**
Acceleration (Time in sec)	5.56	5.55
SkidPad (Time in sec)	5.45	5.42
Autocross (Time in sec)	57.75	56
Endurance (Time in sec)	151	147

5.2 Gears Structural Analysis

The spur gear analysis was done based on the ISO 6336-5 standard for calculating the load capacity of spur and helical gears.[19] To simplify computation effort, the gear analysis software KISSsoft developed by KISSsoft AG was used.[20] Kinematic modeling was also done with the help of KISSsoft simulation.

Access to this software is a major equity challenge. Currently the company sponsors a student version of the software for the UTFR team. However, UTFR might lose access in the future. To mitigate this potential issue, the relevant standards and equations have been identified which the software algorithm is using. Analytical approach can be implemented by the team in the future if the software is not provided.

The most critical safety aspects on the teeth are root and flank safeties. The ISO-6636 5 standard was chosen over the AGMA standards for the bending and contact stress measurements since it is more conservative in safety grading [21]. The stress values at failure were compared to the allowable stress values for the material to determine the factor of safety. The equations below describe the contact (σ_{Hlim}) and bending stress number (σ_{FE}) and safety factor as per ISO-6636 part-5.

The allowable stress value for bending, is the basic bending strength of the un-notched test piece, under the assumption that the material condition (including heat treatment) is fully elastic multiplied by the stress concentration factor

$$\sigma_{FE} = \sigma_{flimit}.Y_{st} \tag{7}$$

The maximum allowable contact stress can be determined graphically based on the material quality. Figure 37 from part-5 of the standard contains the relevant value for medium quality, low carbon steels.

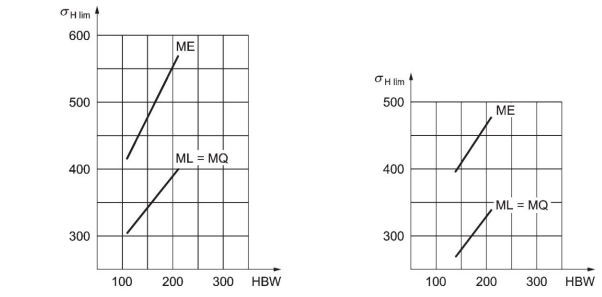

a) Wrought normalized low carbon steels **b) Cast steels**

Key

$\sigma_{H\,lim}$ allowable stress number (contact), N/mm²

HBW surface hardness

Figure 1 — Allowable stress numbers (contact) for wrought normalized low carbon steels and cast steels (attention is drawn to the quality requirements of 6.2)

Figure 37: σ_{Hlim} values based on ISO-6336-5

The design achieved a root safety factor > 2.5 and a flank safety factor > 1.4, well above the 1.2 minimum requirement. To achieve the safety factors, the gears must be heat treated to the specifications as per the heat treatment drawings in Appendix G

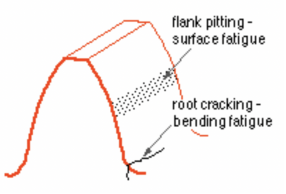

Figure 38: Flank Safety and Root Safety Factor Illustration [22]

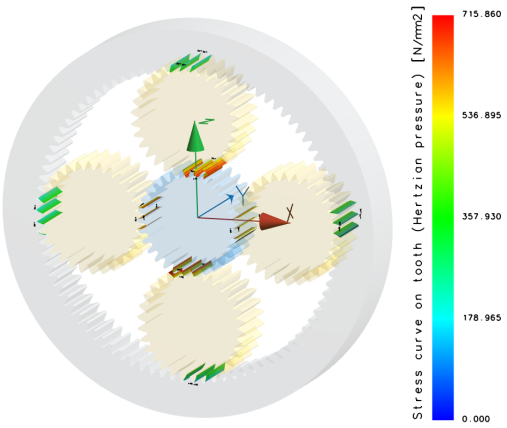

Figure 39: System Teeth Stress

Good engineering practice recommends meeting or exceeding the standards. However it was determined that ISO standards give an overbuilt design which is not ideal for a racing case. Given the low service life of 350 hours per season, the team iterated the design of the gears to further reduce mass.

To reduce mass, 6 holes of 7.5 mm diameter with constant circular pitch between them are drilled along the gear face. Indents of 10 mm on each side were implemented on the gear face as well.

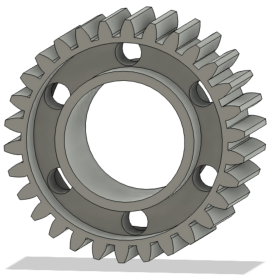

Figure 40: Gear with indent and bore holes

ANSYS simulation was done on the modified gear for stress analysis. It can be seen that the maximum stress on the gear is at $3.79 \times 10^8 Pa$, which is below the maximum stress the gear can withstand, at $7.8 \times 10^8 Pa$ found in Section 4.3.2. In addition, by removing materials off the gears via indents and holes, stress will not concentrate at the holes or the indents.

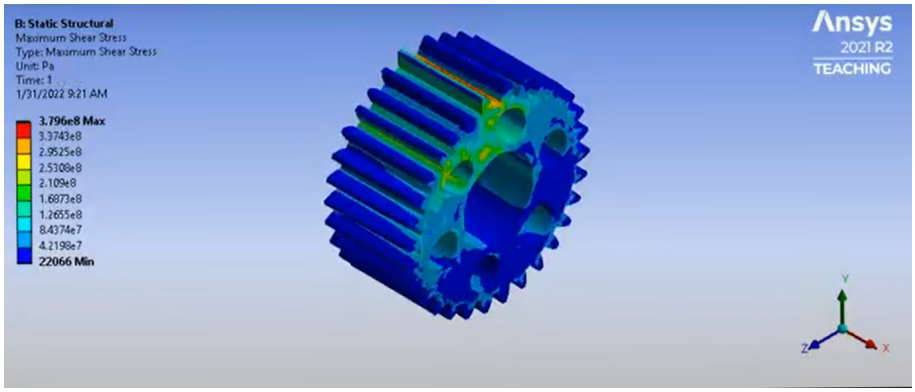

Figure 41: Modified Gear Stress Analysis

The introduction of these weight reduction measures reduce the weight of each gear by 22.77g. With 4 planetary gears within the gearbox, that allows a total weight reduction of 91.08 g. Similar modifications to the sun gear brought down the total weight of the overall design by 100 g.

5.3 Shafts Structural Analysis

The shafts experienced both the Torsional loads from the transmitted torque, and the Bending moment from the forces transmitted via the spur gear mesh. Initially the shafts were sized to transmit the appropriate torque. The diameter of the shaft was designed such that the shear stress due to torsion was below the shear yield stress for AISI 4340 (470 MPa). Equation 8 describes the stresses in the shaft due to torsion. The planet pin is only subjected to bending with no torsion. The stress due to torsion were calculated using the equation below

$$\tau = [K * \frac{T * r}{J}] \tag{8}$$

The stresses due to bending moment were calculated as per the equation below

$$\sigma = [K * \frac{M * y}{I}] \tag{9}$$

Table 17 summarizes the results of the diameter, maximum equivalent stress and deflection in the shafts.

Table 17: Shaft Size

Shaft	**Smallest Diameter (mm)**	**Equivalent Stress (MPa)**	**Deflection (μ m)**
Input Shaft	25	114.852	0
Planet Pin Shaft	20	88.08	11.27
Output Carrier	50	40	0

It was noticeable that due to the additional support from the output carrier, planet pins will be subjected under symmetrically distributed force. Planet pin's deflection will be within the acceptable deflection tolerance for a spur gear mesh i.e (0.003 in). [12]

To avoid stress concentration due to keyway, splines etc, a force fit with shaft tolerance of k6 and hole tolerance of U7 was chosen. The pressure in the given fit was determined by the equation below.

$$P = \frac{0.5\delta}{\frac{r}{E_0}(\frac{r_d^2+r^2}{r_D^2-r^2} + v_D) + \frac{r}{E_i}(\frac{r^2+r_i^2}{r^2-r_i^2} - v_i)} \tag{10}$$

The torque transmitted by the interference fit is given by

$$T = 2 * \pi * \mu * p * l \tag{11}$$

The torque can be calculated as 331 Nm, which is above the requirement of 231 Nm. However, to improve low-cycle fatigue and surface failure, it is recommended to heat treat the shaft to 48RC.

5.4 Kinematic Analysis

Prior to casing and housing designs the rough sized gears with a module of 2mm were modelled using KISSsys to verify kinematics. Figure 42 and 43 show the modeled system on KISSsys and its power flow diagram. The red lines indicate the power flow. The input goes to the sun gear and then is transmitted to the carrier via the planet gears. The ring gear is constrained without rotation.

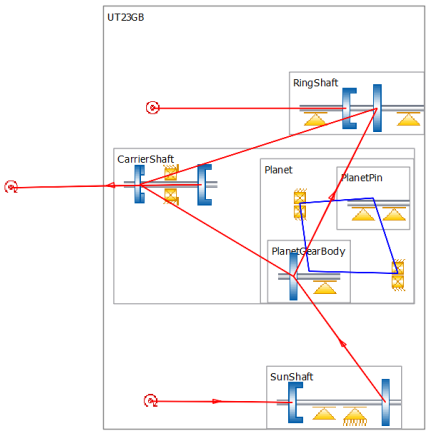

Figure 42: Power Flow Diagram

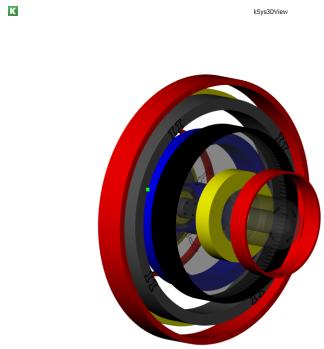

Figure 43: Kinematic Model

The flow of arrows shown in the figure confirms the power-flow with the constrained ring gear. This simulated analysis also matches the analytical results done in Section 4.3.2 on planetary type, showing that no power flow will come out of the fixed ring gear.

5.5 Housing Structural Analysis

An enclosed structure, the Outer Housing, was designed to shield the internal components of the planetary gearbox from dirt, dust, fouling and other contamination. It also protects the interior mechanism from structural stress and/or potential physical, thermal, chemical, biological or radiation related damages from the surrounding environment. Aluminum 6061-T6 was selected as the material of choice due to it's high strength to weight ratio [23], it can be referred to Section 4.2

Initial Design:

As shown in Figure 44, the first iteration of the Outer Housing consisted of one solid aluminum

discs with varying thickness, assembled onto the main body with a total of 8 threaded inserts. The mass of the outer housing is 1.63 kg [Appendix E]

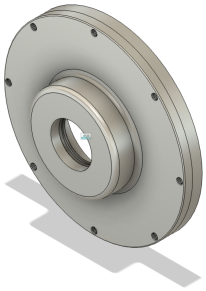

Figure 44: Initial Outer Housing Design

FEA of the Initial Iteration:

Finite Element Analysis is done to verify if the housing can withstand the worst loading condition. When the wheels are stuck, the power flow will be redirected from the motor to the ring gear. As the ring gear is held by the two housings, two housing pieces will experience the same torque output from the motor.

Eqv Von-Mises stress is a value used to determine if a given material will yield or fracture. It is mostly used for ductile materials, such as metals [24]. ANSYS Workbench was utilised to perform Static Structural test in order to calculate the Von-Mises Stress around 8 threaded inserts as shown in Figure 45, when each screw hole is subjected to a force of 995 N [Appendix E], with outer surface being fixed to the chassis. It was observed that each screw hole experienced a maximum stress of 9.2 MPa as shown in Figure 46, which is 30 times lower than the yield strength of Aluminum 6061-T6 (276 MPa) [23]

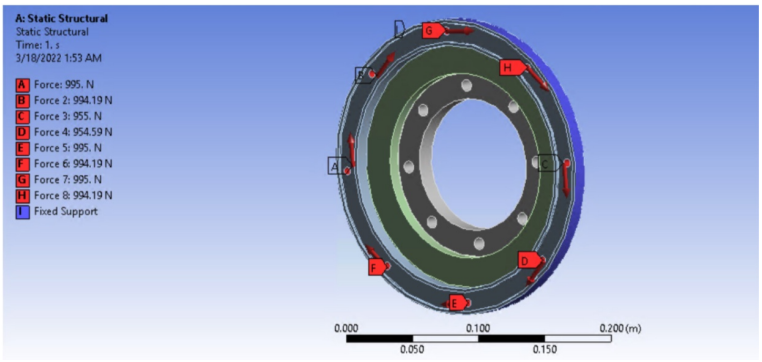

Figure 45: ANSYS Setup for Structural Analysis

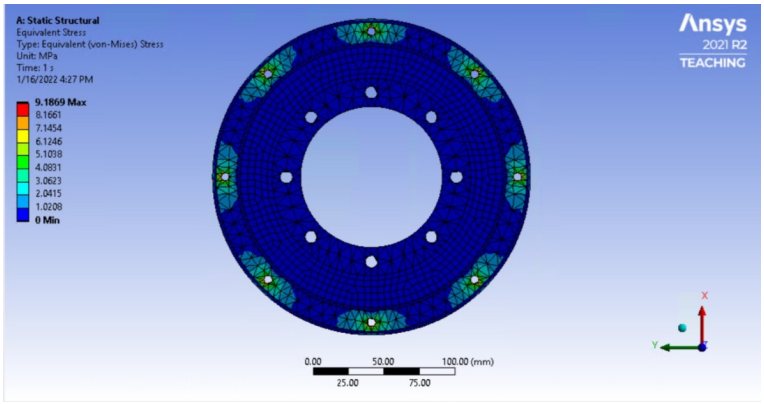

Figure 46: Von-Mises Stress Around Screw Holes

Final Design: Since very low stress was experienced in the vicinity of 8 bolt holes, material was removed in this region as shown in Figure 46. The final mass of the outer housing was reduced from 1.6kg to 1.1 kg. Figure 47 shows the updated assembly with a new outer housing. The other advantage of this design is that it enables more cooling for the gearbox as outer surface area is increased. With a larger surface area, air convection cooling can be more effective to remove the heat from the gearbox.

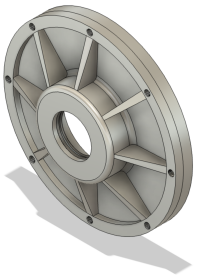

Figure 47: Updated Outer Housing Design

5.6 Lubrication

Amongst the common causes of gearbox failures are wears caused due to metal-on-metal contact, such as galling, abrasion. Therefore, the proper amount of lubricant is critical for the long life of a gearbox. Excessive lubrication however would add to the viscous drag in the gearbox. An optimal mixed lubrication zone is therefore used for lubrication. A. Jackson et al. carried out research in implementing the EHL theory for gear lubrication [25]. The required amount of lubrication is determined by a parameter called specific film thickness (usually ≥ 1) which depends on surface roughness (σ)and thickness of the lubricant(h). The thickness of the lubricant film(h) is based on the geometric factor (G) depending on the type of gearbox, the lubricant parameter (LP), the speed (N), transmitted load (W_t) and contact length (l). The equations below show how the parameters are computed and the results are summarised in Figure 48 and 49

$$\lambda = \frac{h}{\sigma} \tag{12}$$

where

$$\sigma = (\sigma_1^2 + \sigma_2^2)^{\frac{1}{2}} \tag{13}$$

and

$$h = [(G * LP * N * (\frac{W_t}{l})^{-0.148}]^{0.74} \tag{14}$$

It was determined that the pitch line velocity of 8.0 m/s would required a specific film thickness of 1.02. Oil grades from ISO VG-22 to ISO VG-1500 (SAE 75W- SAE 250) were considered and the oil with least viscosity that met the requirements was choose. ISO VG-460 (SAE 140) was the least viscous oil that met the criteria. Figure shows the specific film thickness variation in the sun-planet and planet-internal gear mesh. Table shows the properties of the oils compared

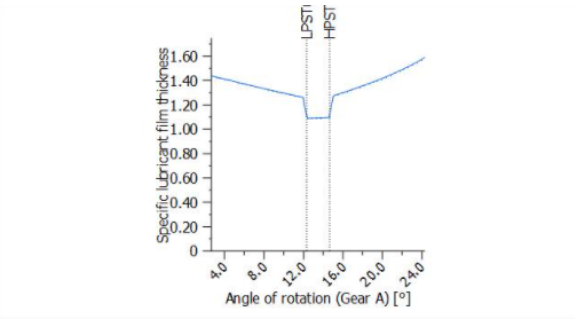

Figure 48: Planet-Sun Gear Mesh

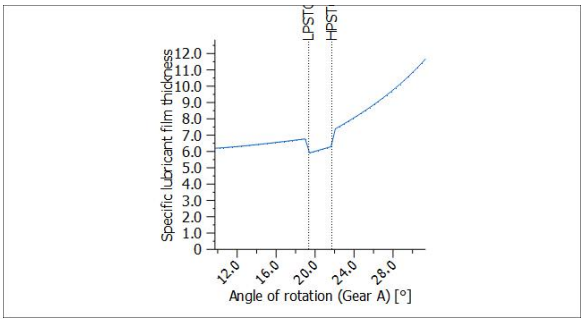

Figure 49: Planet-Internal Gear Mesh

Table 18: Lubrication Selection

ISO Grade	**Viscosity (CentiStokes) at 40°**	**Viscosity (CentiStokes) at 100°**	**Density** (kg/m^3)
32	32	21.9	0.82
46	428	25.5	1
68	520	35.8	1.61
100	525	39.2	1.81
150	525	39.2	1.81
220	525	39.2	1.81
460	525	39.2	1.81

5.7 Cooling

The specific film thickness was calculated based on lubricant properties at a temperature of 40 °C. As the temperature increases the viscosity decreases and the value of the parameter LP decreases. Therefore it is important that the lubricant be maintained at a relatively low temperature.

It was estimated that due to machine element connections such as bearings and gear mesh the design would have an efficiency of 91%. This value can be best estimated for preliminary analysis and it is recommended the client use dyno testing as described in Appendix H to determine it experimentally. Simulation from Optimum lap yielded an average power consumption of 19000 W in autocross. Using an efficiency estimate of 91% the power lost is 1710 W.

In order to evaluate if any additional coolings are required, cooling via air convection was first computed. The gearbox was modelled as a cylinder with D=112 mm in an external forced convection during the autocross race. Using a simulated average race velocity of 16.00 m/s a h value of $68.00 W/m^2K$, equations below describes the Reynolds number, nusselt number and h value calculations. The cooling due to air was estimated to be 108 W which wasn't sufficient.

$$Re = \frac{\rho * V_{avg} * D_h}{\mu} \tag{15}$$

$$Nu = 0.0027 * Re^{0.805} * Pr^{1/3} \tag{16}$$

$$Nu = \frac{h * D_h}{k} \tag{17}$$

$$Q = h * A * \Delta(T) \tag{18}$$

Therefore it is estimated that the cooling load is 1602 W. Since the gear box was oil lubricated which had a high specific heat capacity it was determined best to use splash oil cooling. The mass flow rate was determined using the equation below. An estimated mass flow rate 0.083 kg/sec equivalent to flow rate 0.575 L/min would be require to keep the temperature of the lubricant at approx 30 °.

$$Q = mdot * cp * \delta(T) \tag{19}$$

A suitable oil cooler that could provide 2000 W was selected [26]. The required air flow rate was determined to be 200 CFM. A 5.2" fan from SPAL can be used to provide the required airflow.[27]

In a nutshell, air convection cooling alone can be effective but not sustainable especially during the enduring racing. The temperature of the gearbox with air cooling alone at an enduring racing will increase to $120°C$ based on the calculated power generation. This will decrease the film thickness and increase frictions between components. With an oil cooler recommended, the gearbox is able to maintain the lubricant temperature at 30°.

5.8 Vibration Analysis

The vibration analysis is used to analyze the natural frequency of the entire gearbox and each individual component. The calculated natural frequencies will then be compared to the analyzed forced vibrations to calculate vibration amplitudes. Most machines fail when the external vibration is near its natural frequency, as shown in the figures below. Those external frequency sources can be the chassis's vibration, the nearby motor's vibration, and unbalanced weight on a rotary. When resonance happens, system will vibrate vigorously causing the screws failures, decrease bearing's operational lifespan and can even pose danger to the surrounding people. Thus it's vital to have a system whose natural frequencies are out of the forced vibration frequency range in order for safe operation to take place.

Figure 50: Shaft Failure[28]

Figure 51: Housing Failure[28]

Figure 52: Gear Failure[29]

5.8.1 Natural Frequencies

1. System Analytical Natural Frequency:
The system's natural frequency can be calculated analytically using the methods below:

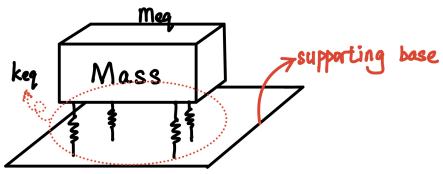

Figure 53: Simplified Vibration Model for the Entire Gearbox

First the equivalent stiffness between the gearbox and the fixture is needed. Based on the simplified model, the total mass of the gearbox is: 14.55kg while the contact material is 4140 Carbon Steel with a Young's Modulus of 190 - 210 GPa[30]. Based on the relationship between the Young's modulus and the spring coefficient

$$k = Y\frac{A}{L} \tag{20}$$

where Y is the Young's Modulus, A is the cross sectional area of the contact part and L is the initial length of the contact part.

As the gearbox will be mounted to the chassis using metal tubes Estimation for the supported area of the gearbox (the total contact area between the gearbox and the chassis) is $1.26\times10^{-4}m^2$ and the length of the contact part is 0.02m. Based on those assumptions, the equivalent spring coefficient is estimated as $k_{eq} = 5 \times 10^8 N/m$:

Natural frequency of the system can be found via:

$$w_n = \sqrt{\frac{k_{eq}}{m_{eq}}} \tag{21}$$

The m_{eq} is the total mass of the system which is equal to 14.55kg. w_n = 9165.15Hz.

2. FEA Modal Analysis on Ansys for Individual Parts
Finite Element analysis is done to analyze the natural frequency of each component at various degree of freedoms. Depending on the external force's orientation and position, the parts will vibrate accordingly. The resulting natural frequencies will then be compared to the forced vibration frequency from Section 6.5.2 for safety compliance.

For the input shaft, as it is mounted directly to the motor via six M8 screws, during simulation, the six screw holes were simulated as the fixed support parts. The resulting lowest natural frequencies from Ansys is given in the table below and an example of the deflection due to vibration deflection is given in the figure.

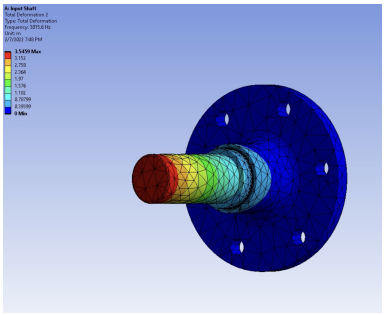

Mode	Frequency(Hz)
1	3014.2
2	3015.6
3	11544
4	11556
5	11631

Figure 54: Modal Analysis on Ansys for Input Shaft

For the input and output carrier, as both carrier pieces are interconnected via four planet pins, the four holes are held stationary in the simulations. The lowest five natural frequencies of the body is shown in the table below, one example of deflection due to the vibration effect is given in the figure.

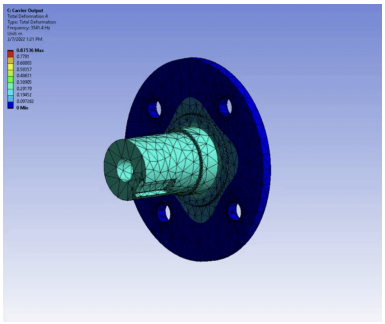

Mode	Frequency(Hz)
1	2354.3
2	2354.6
3	3541.4
4	4703.0
5	4749.2

Figure 55: Modal Analysis on Ansys for Output Carrier

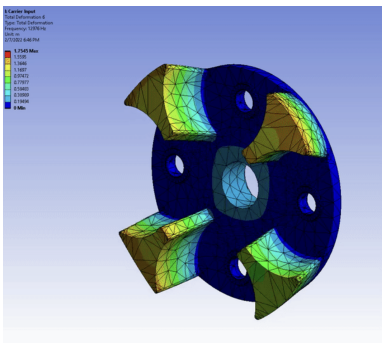

Mode	Frequency(Hz)
1	12423
2	12424
3	12427
4	12434
5	12976

Figure 56: Modal Analysis on Ansys for Input Carrier

Other component's Modal analysis can be found in Appendix K.

5.8.2 Forced Vibrations

The forced vibration frequencies are the frequency of the system or individual part when they are subjected to external forces. Analysis need to be done to test the amplitude amplification and if the gearbox can tolerate the forced vibration under operation. Overall, there are three types of forces that causes the vibrations:

- Unbalanced Weight on the Shafts

- Normal Meshing Between the Gear Teeth
- High-Frequency Impacts Caused by a Local Fault on a Gear Tooth

1. Rotational Vibration Due to Unbalanced Weights:

The unbalanced mass on a rotary system might be caused by the imperfection of rotary parts, existing key-way indents and gear teeth wear-out. This will cause the center of gravity of the rotational object to be offset from the rotational axis, thus leading to vibration.

Assume the off centered unbalanced mass is m, distance between the center of gravity and rotational axis is e, and the rotational speed is ω:

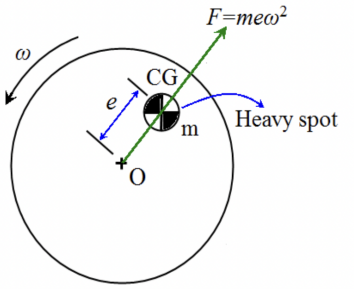

Figure 57: Vibration Induced by Uneven Weight in Rotational Parts Illustration

This gives as the force subjected on the shaft:

$$F = me\omega^2 \tag{22}$$

This equation shows that when there is an unbalanced mass, the force that is subjected onto the supporting bearings or chassis will be high and will increase as the rotational speed increases. To simplify the vibration problem, a single mass Jettcott Rotor Model will be used. As seen from the figure that two ends of the shaft is fixed by two bearings, while the rotary part is simplified into one single mass m with an unbalanced mass m_u.

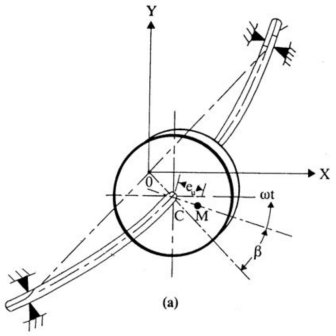

Figure 58: Single Mass Jeffcott Rotor Model [38]

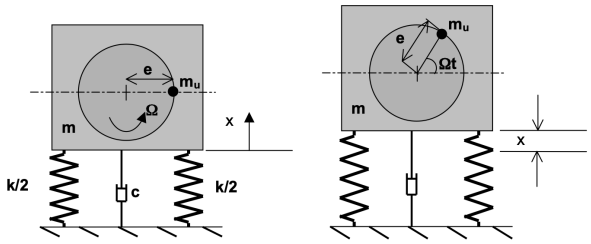

Figure 59: Model of an unbalanced rotating machine, m_u is the unbalanced mass, e is the distance of the unbalanced mass from the rotational axis[31]

$$-kx - cx' = (m - m_u)\frac{d^2x}{dt^2} + m_u\frac{d^2}{dt^2}(x + esin(wt)) \tag{23}$$

The final vibration response can be model as:

$$x = X_0 sin(wt - \phi) \tag{24}$$

Based on this equation, the amplitude and phase angle is calculated as:

$$X_0 = \frac{m_u r^2 e/m}{\sqrt{(1-r^2)^2 + (2\varepsilon r)^2}} \tag{25}$$

$$tan\phi = \frac{2\varepsilon r}{1 - r^2} \tag{26}$$

where $r = \frac{\omega}{\omega_n}$, $w_n = \sqrt{\frac{k}{m}}$, $\varepsilon = \frac{c}{2\sqrt{km}}$
In our design, the only significant unbalanced mass vibration occurs at the output carrier due to the key way indent, as shown in the figure below. the unbalanced mass value is estimated to be around $m_u = 7.84 \times 10^{-3} kg$, the offset distance e = 0.025m, damping ratio for carbon steel $\omega = 0.01$ [33] and the mass of the output carrier m = 2.398kg

At resonance, the vibration amplitude (X_o) reaches the peak. $X_o = \frac{m_u e}{2\varepsilon m} = 4.087 \times 10^{-3} mm$, while the phase angle becomes 90°

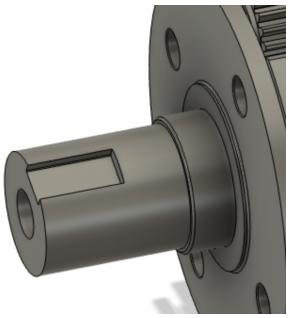

Figure 60: Unbalanced Rotary Part Due to Key-way Indent Illustration

2. Normal meshing between the gear teeth: [34]

The tooth-mesh frequency, also called gear-mesh frequency, is the rate at which gear and pinion

teeth periodically engage [34]. The meshing frequency is in relationship with the input shaft frequency regarding to the equation below:

$$f_{mesh} = f_{input} \times \frac{InputGearTeethNumber}{OutputGearTeethNumber} \tag{27}$$

where f_{mesh} is the meshing frequency, f_{input} is the input frequency from the motor. Since the motor's maximum rotational speed is at 3300rpm (55Hz), $f_{input} = 55Hz$, therefore, $f_{mesh} = 1550Hz$

Vibration frequency due to gear mesh is also simulated on MATLAB, and the resulting graph is shown below (Source Code can be referred to Appendix), where the maximum forced vibration amplitude of the whole gearbox due to the meshing is around 1.5mm.

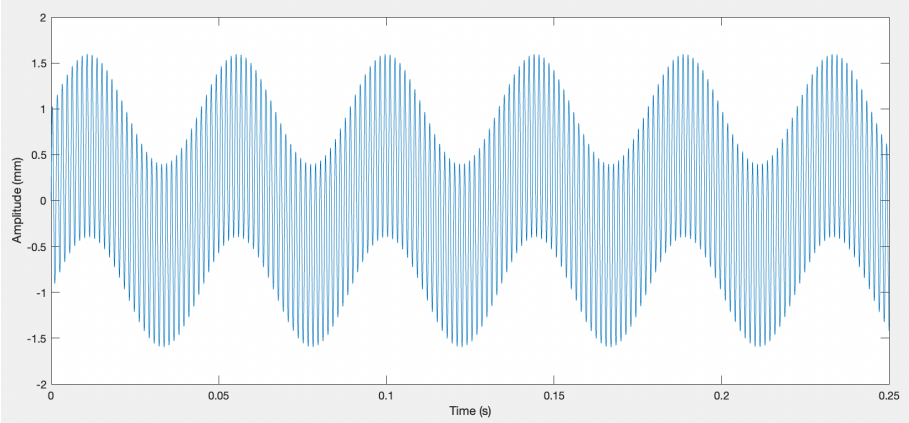

Figure 61: Vibration Due to Gear Mesh Under Normal Conditions

3. High-Frequency Caused by a Local Faulty Gear Tooth:[35]

If one of the gear teeth breaks, it will generate higher frequency at impact due to the shorter duration when teeth are meshed. For example, dents on a tooth will generate high-frequency that will oscillate over the gearbox body.

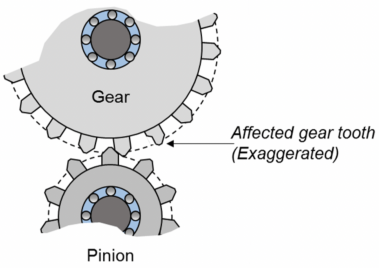

Figure 62: Faulty Teeth Illustration

The local fault causes an impact that has a duration shorter than the duration of tooth mesh. A dent on the tooth surface of the gear generates high-frequency oscillations over the duration of the impact. The frequency of impact is dependent on gearbox component properties and its natural frequencies [34]. We assume a 2kHz impact frequency generated at the span of 0.25ms. Based on this assumption, we can plot the difference between gearbox under normal and faulty working conditions

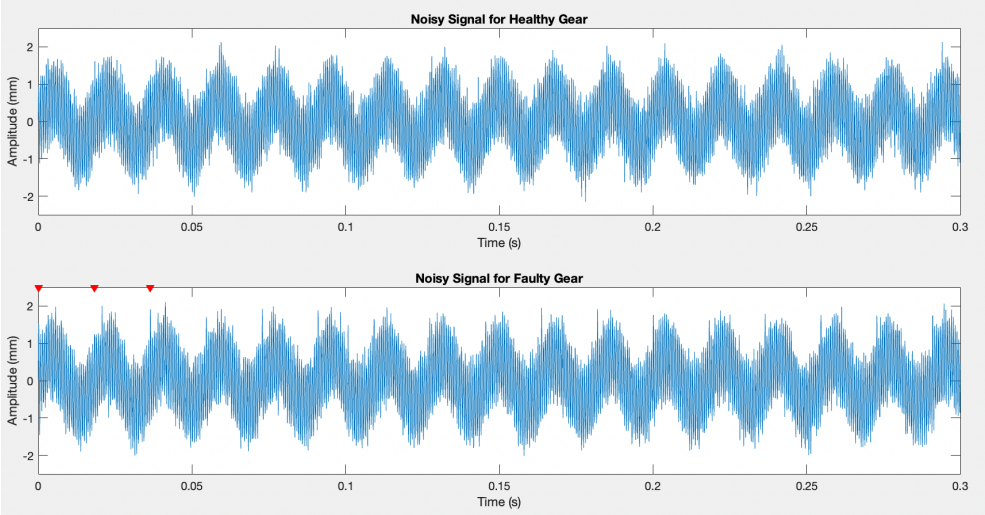

Figure 63: Vibration Response Difference Between Normal Conditions and Faulty Conditions (The three red points are examples showing the spike of the indents)

Furthermore, the power spectrum between the normal conditions and faulty conditions are also analyzed. It can be seen that under faulty condition, the energy spikes periodically, and the estimated periodic frequency is the same as the input rotational frequency at 55Hz. The amplitude of those spikes however is close to 2mm which might cause damages to the bearings and other components.

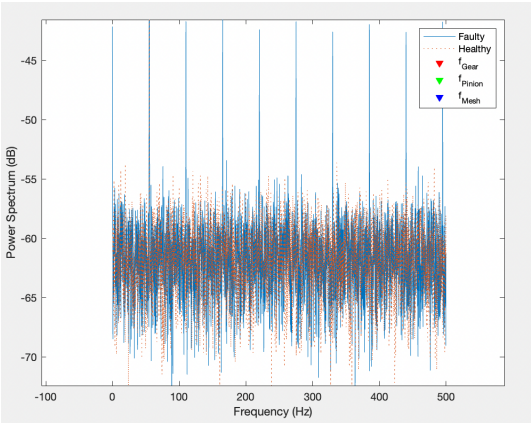

Figure 64: Power Spectrum Difference Between Normal Conditions and Faulty Conditions

In conclusion, both the system natural frequency and the individual component frequency is not in the range of forced vibration frequencies. Under the unbalanced key way rotational vibration conditions, the resulting amplitude is under 0.005mm and can be neglected. Normal gear meshing impact frequency will vibration the system at the frequency of 1550Hz with a maximum amplitude of 1.5mm.

Moreover, it can be concluded that failed individual teeth can result in more severe vibrations and unwanted energy peaks inside the gearbox. When there are signs of wears and tears inside the gearbox, timely maintenance is required to prevent further vibration damages.

5.9 Lifecycle Analysis

The lifecycle analysis shows an overview of the environmental impacts of our design. Environmental impacts in terms of CO_2 kg eq. of the overall design is shown in the graph below.

All materials used for components are considered to be made from virgin sources, meaning no percentage of the component is made from recycled materials. All components are assumed to be either recycled or reused at their end of life. This is in line with UTFR practices.

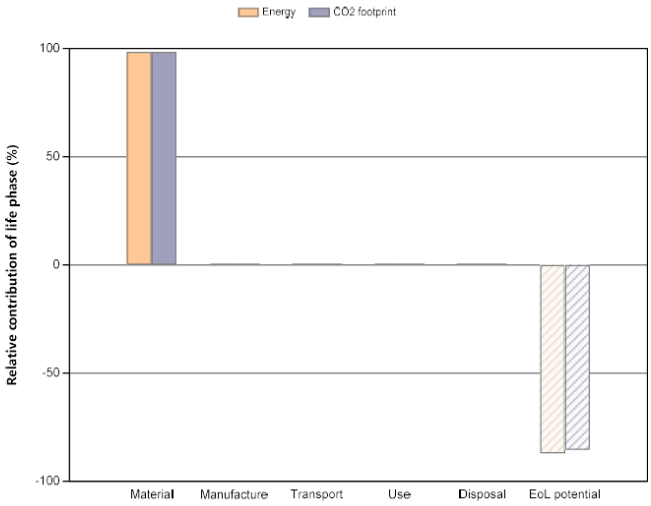

Figure 65: Energy and CO_2 Summary of the design

Table 22: Energy and CO_2 Cost Breakdown

Phase	**Energy(MJ)**	**Energy(%)**	CO_2**Footprint(kg)**	CO_2**Footprint(%)**
Material	859	98.6	59.9	98.6
Manufacture	0.448	0.1	0.0336	0.1
Transport	2.69	0.3	0.194	0.3
Use	3.32	0.4	0.2	0.3
Disposal	5.7	0.7	0.399	0.7
Total (for first life)	872	100	60.7	100
End of Life Potential	-756		-51.7	

It is assumed that the gearbox manufacturing and transportation is done by one of UTFR's stakeholders, namely one of their sponsors. Therefore, all the materials and components for the gearbox are sourced within Ontario. Finally, 120km radius in range is assumed as the transportation distance.

However, as per Figure 65, a substantial increase in distance will not have a dramatic impact on the energy and emissions percentage for that life-cycle stage. This is because the material themselves account for almost all the energy and CO_2 emissions. The usage phase of the product life cycle understandably occupies less portion of the total emissions.

The vehicle travels less than 100 km for each event. Since it is an EV vehicle, overall emission from the vehicle is less than what it would be for an Internal Combustion Engine vehicle.

The end of life phase is when the entire vehicle has to be redesigned or modified further depending on its performance from previous events. In this case, most of the components from the gearbox can be reused, namely the gears and bearings. The housing and other non critical components can be recycled by smelting and remolded into other parts.

The end of life phase potential savings recovers almost all of the CO_2 emissions from the design as well as almost all of the energy invested into the design as shown in the Table above.

6 Capstone Showcase Prototype

The initial plan to design and construct a metal gearbox that could be tested and used for the UT23 vehicle couldn't proceed due to pandemic disruptions and the high cost.

After consultations, a full scale 3D printed prototype with all machine elements was assembled. This prototype was tested for functionality and determining any assembly issues caused by tolerance stack-up. The prototype was able to achieve the intended function of transmitting motion from input to output and modify it suitable to reduce speed. The team also tested the prototype for sealing and noted no major oil leak.On leaving the design however there was a slight trickle near the bottom. The O-ring design can be improved by using a standard gland sizing method for face sealing using the machinery's handbook.[37] The design was assembled at the team's workshop using the available tools within 1 hour meeting the assembly time objective.

In order to take advantage of the 3D printed parts, one side of the housing had a quarter cutout to demonstrate the internal mechanical movements.

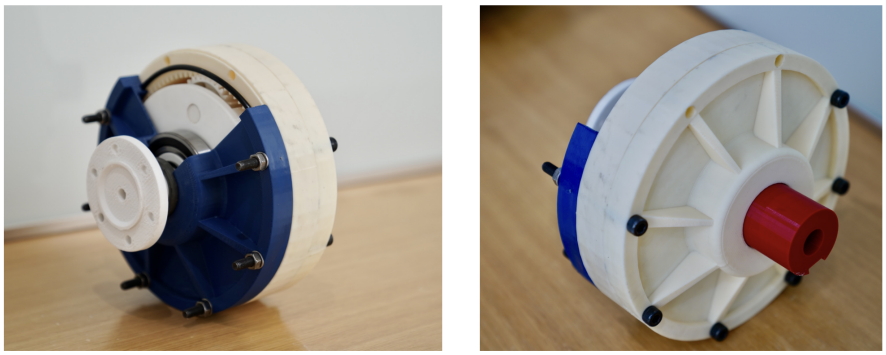

Figure 66: 3D Printed Assembled Prototype

The 3D Printed Prototype was used to verify the following objectives for the project:

- Overall dimensional sizing

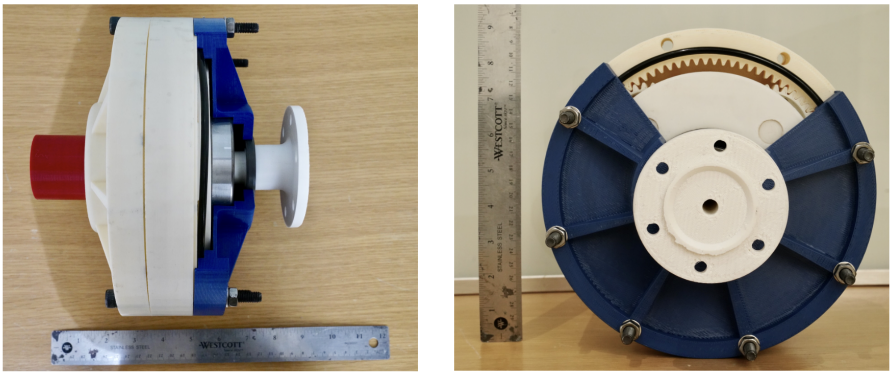

Figure 67: 3D Printed Assembled Dimensions

- Test the gear ratio The degree of rotation from the output shaft caused by one full revolution of the input shaft was recorded and determined to be equal to the gear ratio.

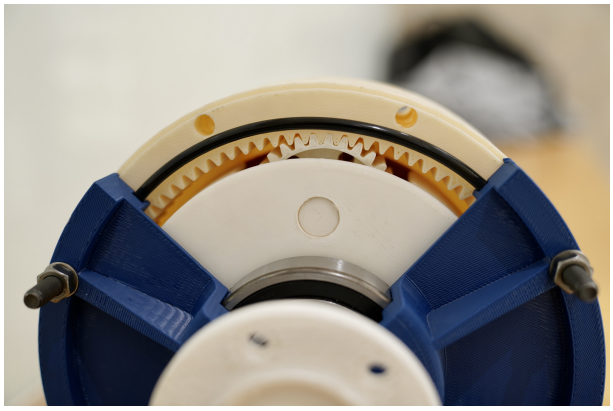

Figure 68: Teeth Fitting Showcase

- Document and time the assembly process (As shown in the Appendix H.8)

  During assembly, the team recorded the assembly time and documented the assembly process for guidance.

- Check the oil seal

  Using the cutout on the housing piece, the sealing was tested by pouring lubrication oil inside and check for leakage.

- Qualitatively determine the effect of adding lubrication

  The torque needed to rotate the gearbox was qualitatively compared before and after the lubrication is applied.The gearbox operated much smoother after lubrication.

7 Conclusions and Future Work

In conclusion, the final design meets the two primary functions and was the most compact solution amongst the compared alternatives. Further coupling to the chain and sprocket ratio provides flexibility to adjust the final drive ratio and makes the design compatible with the Drexler differential. The design will improve the car's performance in the dynamic events such as the endurance race and help the team perform better in competition

Testing on the dynamo-meter is recommended to determine the final efficiency of the design and determine if any other changes such as adjustments to the cooling system need to be made before implementation. The gearbox is built for a service life of 1000 hours and can be reused for two competition seasons in order to make the high investment associated with manufacturing justifiable.

References

[1] 2021 rules release. [Online]. Available: https://www.fsaeonline.com/cdsweb/app/NewsItem.aspx?NewsItemID=51cf7622-651e-4b57-8c9c-e0391bc08edc. [Accessed: 27-Sep-2021].

[2] "All Standards by Product", NEMA, 2021. [Online]. Available: https://www.nema.org/standards/all-standards-by-product/Index/8ca04bb4-8b57-4d99-b75b-42acd1342470/. [Accessed: 16- Sep- 2021].

[3] "Powertrain — Highlander Racing - FSAE", Highlander Racing - FSAE, 2021. [Online]. Available: https://www.highlanderracing.org/powertrain. [Accessed: 29- Sep- 2021].

[4] Wisconsinracing.org, 2021. [Online]. Available: https://www.wisconsinracing.org/wp-content/uploads/2020/10/WR-217e_Rear_Drivetrain_Design_Overv iew.pdf. [Accessed: 29-Sep- 2021].

[5] N. Daniel Rhyoo, "Illini Formula Electric", Illiniformulaelectric.com, 2021. [Online]. Available: https://illiniformulaelectric.com/. [Accessed: 29- Sep- 2021].

[6] "REV0 — Penn Electric Racing", Penn Electric Racing, 2021. [Online]. Available: https://www.pennelectricracing.com/rev0. [Accessed: 29- Sep- 2021]

[7] "Engine Gear Oil - Recommended Viscosity vs. Outside Temperature", Engineeringtoolbox.com, 2022. [Online]. Available: https://www.engineeringtoolbox.com/engine-gear-oil-viscosity-temperature-limits-d_1545.html. [Accessed: 01- Apr- 2022].

[8] "Spur Gears", Drivetrainhub.com, 2022. [Online]. Available: https://drivetrainhub.com/notebooks/gears/geometry/Chapter%202%20-%20Spur%20Gears.html. [Accessed: 01- Apr- 2022].

[9] "Herringbones 101", Geartechnology.com, 2022. [Online]. Available: https://www.geartechnology.com/blogs/1-gear-talk-with-chuck/post/19724. [Accessed: 01- Apr- 2022].

[10] "Helical gear set - helical gear,helical gear design,double helical gear,helical gear calculations,helical gear calculation,helical bevel gear,helical gear applications,helical gear definition,crossed helical gear", Bestagear.com, 2022. [Online]. Available: http://www.bestagear.com/helical_gear/helical_gear_set.html. [Accessed: 01- Apr- 2022].

[11] G. Knowledge, G. Reference and G. Systems, "Gear Systems — KHK Gears", KHK Gears, 2022. [Online]. Available: https://khkgears.net/new/gear_knowledge/gear_technical_reference/gear_systems.html. [Accessed: 31- Mar- 2022].

[12] R. BUDYNAS, SHIGLEY'S MECHANICAL ENGINEERING DESIGN. [Place of publication not identified]: MCGRAW-HILL EDUCATION, 2019.

[13] :"A gear element in a wind-turbine gearbox", ScienceDirect, 2022. [Online]. Available: https://www.sciencedirect.com/topics/engineering/pressure-angle. [Accessed: 01- Apr- 2022].

[14] "Calculations of Internal Gears and The Fundementals of Helical Gears - SDPSI", SDP/SI Small Mechanical Components, 2022. [Online]. Available:https://www.sdp-si.com/resources/elements-of-metric-gear-technology/page3.php. [Accessed: 31- Mar- 2022].

[15] D. Collins, "Gearbox lubrication: What are the best methods?", Motioncontroltips.com, 2022. [Online]. Available: https://www.motioncontroltips.com/gearbox-lubrication-best-methods/. [Accessed: 01- Apr- 2022].

[16] "Full Thread vs. Partial Thread Screws and Bolts", FMW Fasteners, 2022. [Online]. Available: https://www.fmwfasteners.com/en-ca/blogs/blog/full-thread-vs-partial-thread-screws. [Accessed: 02- Apr- 2022]

[17] "OptimumLap — OptimumG", Optimumg.com, 2022. [Online]. Available: https://optimumg.com/product/optimumlap/. [Accessed: 01- Apr- 2022].

[18] "228 (109kW — 230Nm) - EMRAX", EMRAX, 2022. [Online]. Available: https://emrax.com/e-motors/emrax-228/. [Accessed: 01- Apr- 2022].

[19] Calculation of load capacity of spur and helical gears. Part 5: Strength and quality of materials. Place of publication not identified: International Organization for Standardization, 2016.

[20] "Home", KISSsoft AG, 2022. [Online]. Available: https://www.kisssoft.com/en. [Accessed: 01- Apr- 2022].

[21] Geartechnology.com, 2022. [Online]. Available: https://www.geartechnology.com/ext/ resources/issues /0718x/gear-rating.pdf. [Accessed: 01- Apr- 2022].

[22] www-mdp.eng.cam.ac.uk. 2022. DANotes: Spur gears: Failure and reliability. [online] Available at: http://www-mdp.eng.cam.ac.uk/web/library/enginfo/textbooks_dvd_only/DAN/gears/failure/failure.html [Accessed 26 March 2022].

[23] "MatWeb - The Online Materials Information Resource." https://www.matweb.com/errorUser.aspx?msgid=2ckck=nocheck (accessed Apr. 01, 2022).

[24] "What is Von Mises Stress in FEA? — SimWiki — SimScale." https://www.simscale.com/docs/simwiki/fea-finite-element-analysis/what-is-von-mises-stress/ (accessed Apr. 01, 2022).

[25] A. Jackson and C. . Rowe, "Application of EHL theory to gear lubrication," SAE technical paper series, 1980, doi: 10.4271/800670

[26] "Setrab 10-Row, Series 1 Oil Cooler", Improvedracing.com, 2022. [Online]. Available: https://www.improvedracing.com/setrab-10-row-series-1-oil-cooler.html. [Accessed: 01- Apr- 2022].

[27] V. 5.2quot;P/12V/SUM, "VA31-A101-46A * 5.2"P/12V/SUM — SPAL Automotive USA", Spalusa.com, 2022. [Online]. Available: https://www.spalusa.com/products/fans/5_2/va31-a101-46a-12-5-2-7-p-3-12v-3-sum-30103011?returnurl=%2fproducts%2ffans%2f5_2%2f. [Accessed: 01- Apr- 2022].

[28] Daytonclutch.com. 2022. Driveline Failures and Vibrations — Dayton Clutch and Joint. [online] Available at: https://daytonclutch.com/driveline/failures¿ [Accessed 28 March 2022].

[29] Drvconsulting.com. 2022. Torsional Failures — Vibration — Vibration Analysis. [online] Available at: http://www.drvconsulting.com/torsional_failures.html [Accessed 28 March 2022].

[30] "4140", Kloeckner Metals Corporation, 2022. [online]. Available at: https://www.kloecknermetals.com/products/plate/grades/4140-steel/. [Accessed 28 March 2022].

[31] Mechengdesign.co.uk, 2022. [Online]. Available: http://mechengdesign.co.uk/ PlannedWeb/mech226/rotunb2.pdf. [Accessed: 28- Mar- 2022].

[32] Liu, Dabiao Peng, Kai He, Yuming. (2016). Direct measurement of torsional properties of single fibers. Measurement Science and Technology. 27. 10.1088/0957-0233/27/11/115017.

[33] "Viscous Damping Ratios for Different Systems and Materials - 2016 - SOLIDWORKS Help", Help.solidworks.com, 2022. [Online]. Available:https://help.solidworks.com/2016/english/solidworks/cworks/r_viscous_damping_ratios.htm. [Accessed: 01- Apr- 2022].

[34] "Frequencies of a gear assembly", Power-MI, 2022. [Online]. Available: https://power-mi.com/content/frequencies-gear-assembly. [Accessed: 30- Mar- 2022].

[35] 2022. [Online]. Available: https://www.mathworks.com/help/signal/ug/vibration-analysis-of-rotating-machinery.html. [Accessed: 29- Mar- 2022].

[36] V. Fedák, P. Záskalický, and Z. Gelvanič, "Analysis of Balancing of Unbalanced Rotors and Long Shafts using GUI MATLAB", in MATLAB Applications for the Practical Engineer. London, United Kingdom: IntechOpen, 2014 [Online]. Available: https://www.intechopen.com/chapters/46862 doi: 10.5772/58378

[37] Oberg, M. Jones and Horton, Machinerys Handbook. New York: Industrial Press, Incorporated, 2004.

[38] Dyrobes.com, 2022. [Online]. Available: https://dyrobes.com/wp-content/uploads/2015/09/Understanding-Amplitude-Phase-In-Rotating-Machinery_linked.pdf. [Accessed: 28- Mar- 2022].

[39] Planetary Gearbox Gear Ratio Calculation, 2022. [Online]. Available: https://www.youtube.com/watch?v=ARd-Om2VyiE. [Accessed: 31- Mar- 2022].

Appendices

A EMRAX Motor Efficiency

This section gives an estimate of the best gear ratio for the motor to operate in the high efficiency range.

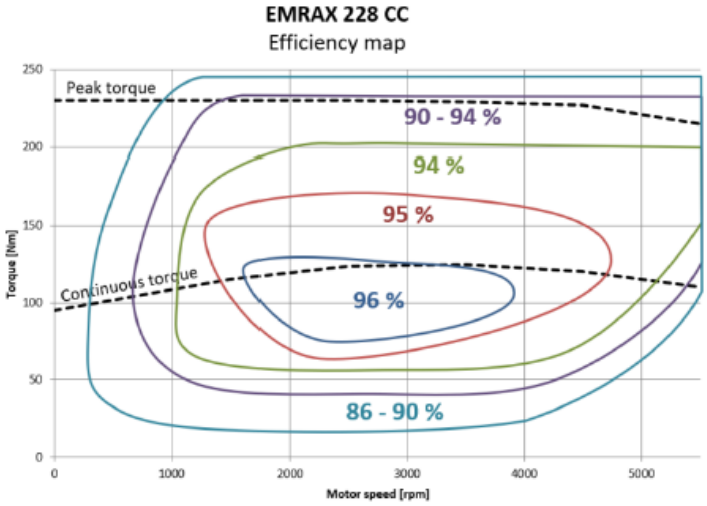

Figure 69: EMRAX Efficiency Map

As seen in Figure 69 the motor outputs the best performance in the RPM ranges 1700-3200 with the continuous torque curve.

During races the car is estimated to operate in the speed range 45 km/h to 65 km/h. Given the wheel radius to be 0.22.

Circumference = $2\pi r$ =1.382 m

Speed= 12.5 m/s - 18.0m/s

Rotations/ sec = 9.04 rotations/sec - 13.02 rotations/sec

Rotations/ min = 542 rotations/min - 781.2 rotations/ min

RPM range with a final drive of 4.0 = 425 RPM - 800 RPM

Therefore the required ratio falls well within the operating range of best performance

B Weather Data

Table 23: Weather Data Breakdown

Month	**Max/Min Temperature ($^\circ C$)**	**Average Daily Max/Min Temperature ($^\circ C$)**	**Average Precipitation (mm)**
March	18.4, -10.9	-2.5	66.1
April	14.8, -4.8	3.12	69.6
May	31, -4.7	11.20	73.3
June	32.1, 7.9	15.24	71.5
July	32.5, 15.3	18.28	67.5

C Weighted Decision Matrix

Table 24: Weighted Decision Matrix

Criteria	Weight	Bevel Gearbox	Spur Gearbox	Planetary Gearbox
Mass and Moment of Inertia	25%	20	80	80
Cost	25%	80	80	60
Compactness	16%	40	60	100
Safety Factor	14%	60	80	100
Gear Ratio	100	100	100	100
Dynamics	10%	50	80	100
Total (Weight $\star Score$)	100%	54.8	78.8	85

Table 25: Justification for Decision Matrix Rubric

Percentages	**Descriptions**
0%	Do not meet the objective at all
20%	Meet the objectives very weakly
40%	Meet the objectives somewhat
60%	Mostly meet the objectives
80%	Meet the objectives strongly
100%	Outstanding with respect to the objectives

Important specifications of the designs in accordance with the objectives are compared. Higher point means better performance. Higher weight means more important objective

https://www.overleaf.com/project/61e4398866cd5fd0258b68b6

Table 26: Cost Breakdown

Part	Cost
Gears& Heat Treatment	$1521.00
Inner Housing	$483.55
Outer Housing	$482.20
Inner Carrier	$701.39
Outer Carrier	$667.84
Input Shaft	$454.14
Planet Shaft	$173.43
Fasteners & Bearings	$308.33
Carrier Bearings	$295.14
Total	$5086.02

D Cost and Key Parameters

The table below shows the cost breakdown. Prices are subject to change based on raw material and labour costs

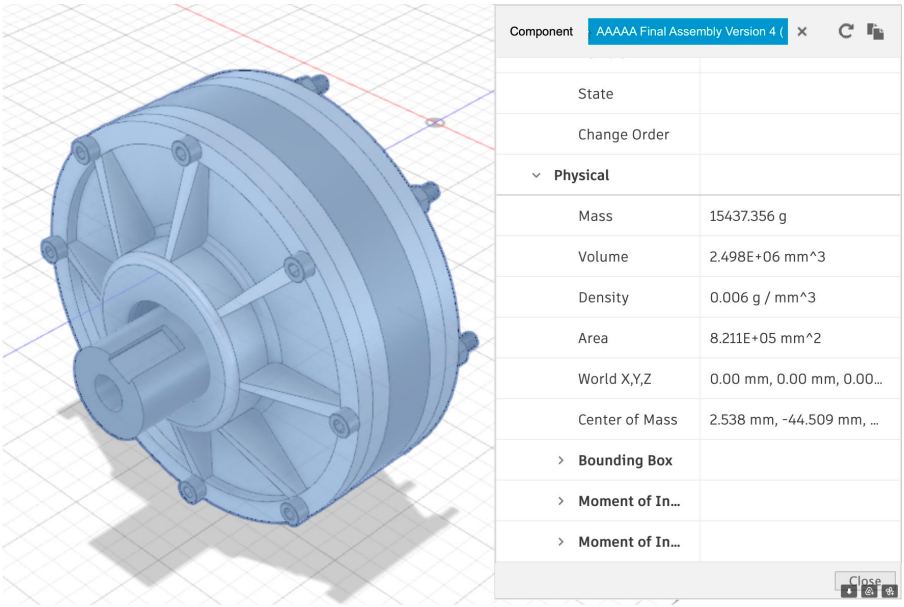

Figure 70: GearBox Specifications

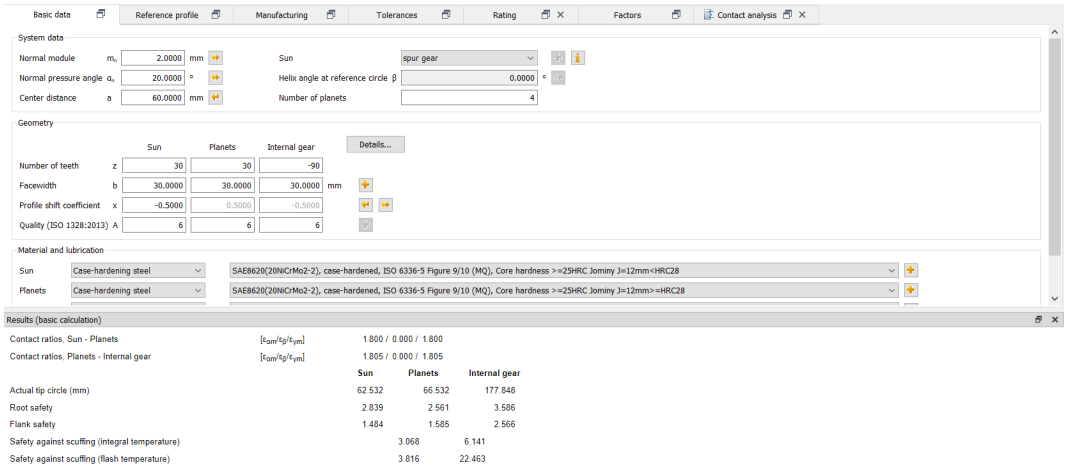

Figure 71: Root Flank Safety and Gear Ratio Data

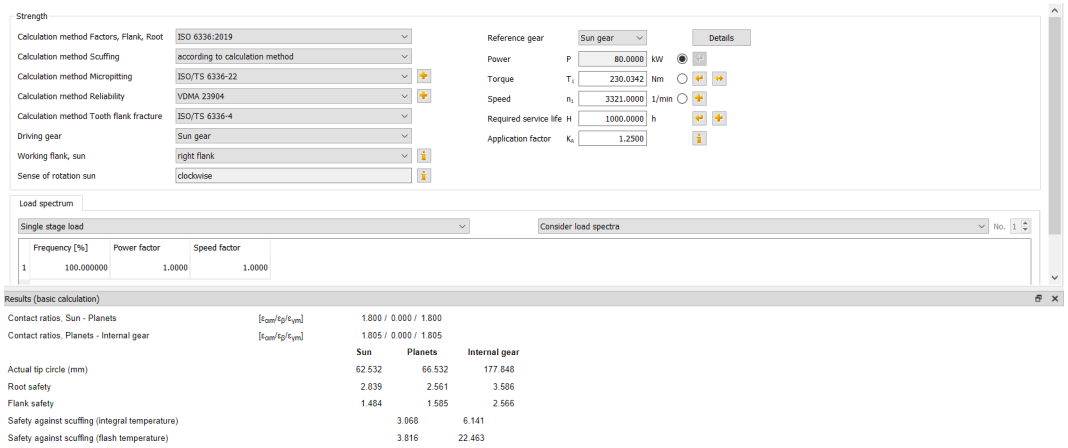

Figure 72: Service Life

E Housing

The Outer Housing is made out of Al-6061-T6, which has a density of 3 g/cm^3

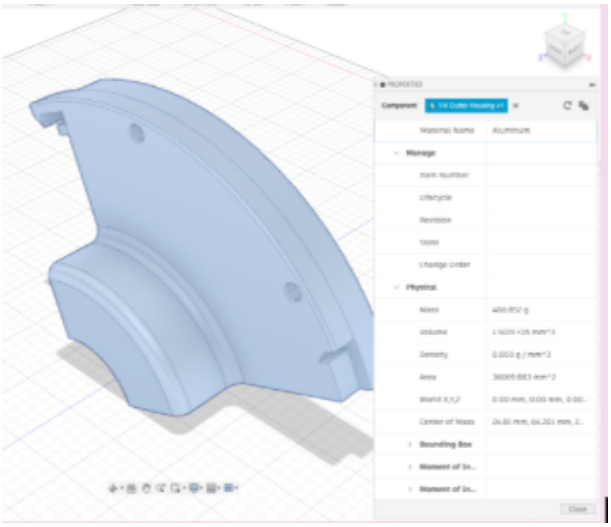

Figure 73: Properties of the initial Outerhousing evaluated using Fusion 360 'Material Properties' feature.

Calculation of force per screw (960 N):

$$\begin{aligned} Applied\,Torque &= 920N.m \\ Radius\,Outerhousing &= 60mm \\ Force &= 920/0.060 = 7666.66N \\ Force\,per\,screw &= 7666.66/8 = 960N \end{aligned}$$

Figure 74: Force Experienced on each threaded insert.

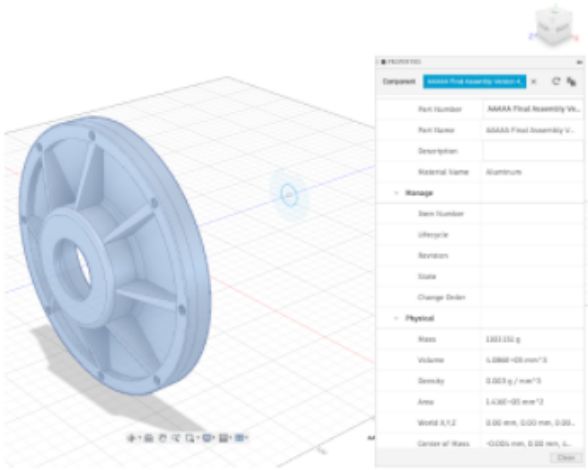

Figure 75: Properties of the updated Outerhousing evaluated using Fusion 360 'Material Properties' feature.

F Lifecycle Analysis

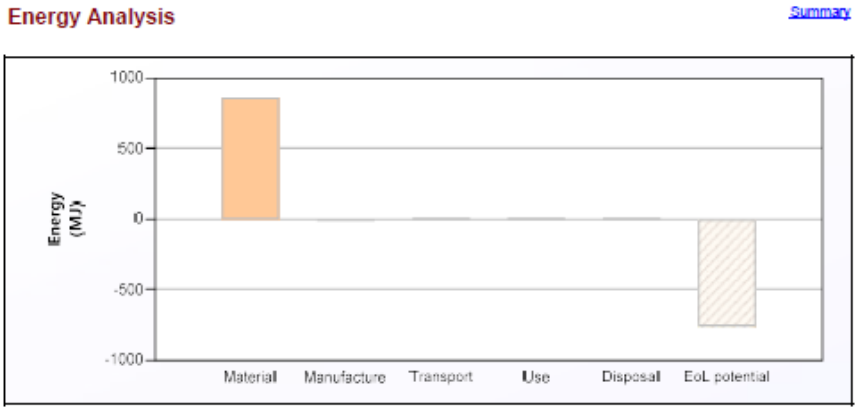

	Energy (MJ/year)
Equivalent annual environmental burden (averaged over 1 year product life):	872

Figure 76: Energy Consumption per lifecycle phase of the design

Detailed breakdown of individual life phases

Material: Summary

Component	Material	Recycled content* (%)	Part mass (kg)	Qty.	Total mass processed** (kg)	Energy (MJ)	%
Output Carrier	Low alloy steel, AISI 4340, oil quenched & tempered at 650°C	Virgin (0%)	2.4	1	2.4	78	9.1
Outer Housing	Aluminum, 6061, T4	Virgin (0%)	1.2	1	1.2	2.3e+02	27.0
Input Shaft	Low alloy steel, AISI 4340, oil quenched & tempered at 650°C	Virgin (0%)	0.84	1	0.84	27	3.2
Inner Housing	Aluminum, 6061, T4	Virgin (0%)	1.1	1	1.1	2.2e+02	25.3
Planet Shaft	Low alloy steel, AISI 4340, oil quenched & tempered at 650°C	Virgin (0%)	0.12	4	0.49	16	1.8
Inner Carrier	Low alloy steel, AISI 4340, oil quenched & tempered at 650°C	Virgin (0%)	2.7	1	2.7	87	10.1
Planet Gear	Low alloy steel, SAE 8630, cast, quenched & tempered	Virgin (0%)	0.29	4	1.1	37	4.3
Sun Gear	Low alloy steel, SAE 8630, cast, quenched & tempered	Virgin (0%)	0.55	1	0.55	18	2.1
Ring Gear	Low alloy steel, SAE 8630, cast, quenched & tempered	Virgin (0%)	4.6	1	4.6	1.5e+02	17.2
Total				15	15	8.6e+02	100

*Typical: Includes 'recycle fraction in current supply'

**Where applicable, includes material mass removed by secondary processes

Figure 77: Energy Consumption per Lifecycle Phase of the Design

Manufacture:

Summary

Component	Process	% Removed	Amount processed	Energy (MJ)	%
Bolts	Fasteners, small	-	16	0.45	100.0
Total				**0.45**	**100**

Transport:

Summary

Breakdown by transport stage

Stage name	Transport type	Distance (km)	Energy (MJ)	%
Supplier run	14 tonne (2 axle) truck	1.2e+02	2.7	100.0
Total		**1.2e+02**	**2.7**	**100**

Breakdown by components

Component	Mass (kg)	Energy (MJ)	%
Output Carrier	2.4	0.44	16.2
Outer Housing	1.2	0.21	7.8
Input Shaft	0.84	0.15	5.6
Inner Housing	1.1	0.2	7.3
Planet Shaft	0.49	0.089	3.3
Inner Carrier	2.7	0.48	17.9
Planet Gear	1.1	0.21	7.6
Sun Gear	0.55	0.099	3.7
Ring Gear	4.6	0.82	30.6
Total	**15**	**2.7**	**100**

Figure 78: Energy Consumption of the Manufacture and Transport Life Phase of the Design

Use:

Summary

Mobile mode

Fuel and mobility type	Electric - family car
Country of use	World
Product mass (kg)	15
Distance (km per day)	30
Usage (days per year)	20
Product life (years)	1

Relative contribution of static and mobile modes

Mode	Energy (MJ)	%
Static	0	
Mobile	3.3	100.0
Total	3.3	100

Breakdown of mobile mode by components

Component	Energy (MJ)	%
Output Carrier	0.54	16.2
Outer Housing	0.26	7.8
Input Shaft	0.19	5.6
Inner Housing	0.24	7.3
Planet Shaft	0.11	3.3
Inner Carrier	0.6	17.9
Planet Gear	0.25	7.6
Sun Gear	0.12	3.7
Ring Gear	1	30.6
Total	3.3	100

Figure 79: Energy Consumption of the Use Phase of the Design

Disposal:

Summary

Component	End of life option	% recovered	Energy (MJ)	%
Output Carrier	Reuse	100.0	0.48	8.5
Outer Housing	Recycle	100.0	0.81	14.3
Input Shaft	Reuse	100.0	0.17	2.9
Inner Housing	Recycle	100.0	0.76	13.4
Planet Shaft	Recycle	100.0	0.34	6.0
Inner Carrier	Recycle	100.0	1.9	32.9
Planet Gear	Reuse	100.0	0.23	4.0
Sun Gear	Reuse	100.0	0.11	1.9
Ring Gear	Reuse	100.0	0.91	16.0
Total			5.7	100

EoL potential:

Component	End of life option	% recovered	Energy (MJ)	%
Output Carrier	Reuse	100.0	-78	10.4
Outer Housing	Recycle	100.0	-1.9e+02	25.4
Input Shaft	Reuse	100.0	-27	3.6
Inner Housing	Recycle	100.0	-1.8e+02	23.9
Planet Shaft	Recycle	100.0	-12	1.5
Inner Carrier	Recycle	100.0	-64	8.4
Planet Gear	Reuse	100.0	-37	4.9
Sun Gear	Reuse	100.0	-18	2.4
Ring Gear	Reuse	100.0	-1.5e+02	19.5
Total			-7.6e+02	100

Figure 80: Energy Consumption of the Disposal and End Of Life Phase of the Design

CO2 Footprint Analysis

Summary

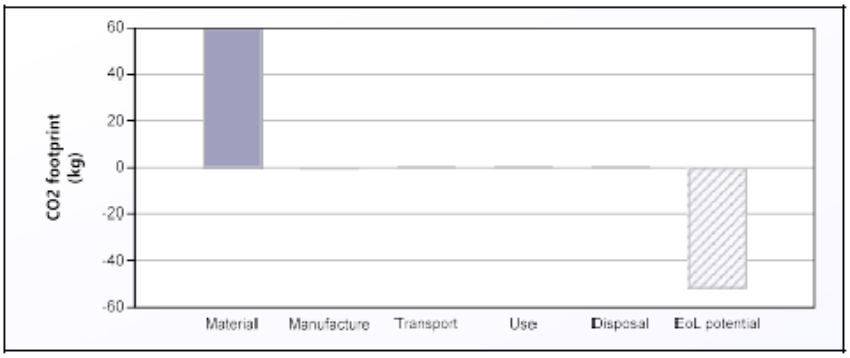

	CO2 (kg/year)
Equivalent annual environmental burden (averaged over 1 year product life):	60.7

Figure 81: CO_2 Emission per lifecycle phase of the design

Material:

Summary

Component	Material	Recycled content* (%)	Part mass (kg)	Qty.	Total mass processed** (kg)	CO2 footprint (kg)	%
Output Carrier	Low alloy steel, AISI 4340, oil quenched & tempered at 650°C	Virgin (0%)	2.4	1	2.4	5.7	9.6
Outer Housing	Aluminum, 6061, T4	Virgin (0%)	1.2	1	1.2	15	25.6
Input Shaft	Low alloy steel, AISI 4340, oil quenched & tempered at 650°C	Virgin (0%)	0.84	1	0.84	2	3.3
Inner Housing	Aluminum, 6061, T4	Virgin (0%)	1.1	1	1.1	14	24.1
Planet Shaft	Low alloy steel, AISI 4340, oil quenched & tempered at 650°C	Virgin (0%)	0.12	4	0.49	1.2	1.9
Inner Carrier	Low alloy steel, AISI 4340, oil quenched & tempered at 650°C	Virgin (0%)	2.7	1	2.7	6.4	10.6
Planet Gear	Low alloy steel, SAE 8630, cast, quenched & tempered	Virgin (0%)	0.29	4	1.1	2.7	4.5
Sun Gear	Low alloy steel, SAE 8630, cast, quenched & tempered	Virgin (0%)	0.55	1	0.55	1.3	2.2
Ring Gear	Low alloy steel, SAE 8630, cast, quenched & tempered	Virgin (0%)	4.6	1	4.6	11	18.1
Total				15	15	60	100

*Typical: Includes 'recycle fraction in current supply'

**Where applicable, includes material mass removed by secondary processes

Figure 82: CO_2 Emission per Component of the design

Manufacture:

Summary

Component	Process	% Removed	Amount processed	CO2 footprint (kg)	%
Bolts	Fasteners, small	-	16	0.034	100.0
Total				0.034	100

Transport:

Summary

Breakdown by transport stage

Stage name	Transport type	Distance (km)	CO2 footprint (kg)	%
Supplier run	14 tonne (2 axle) truck	1.2e+02	0.19	100.0
Total		1.2e+02	0.19	100

Breakdown by components

Component	Mass (kg)	CO2 footprint (kg)	%
Output Carrier	2.4	0.031	16.2
Outer Housing	1.2	0.015	7.8
Input Shaft	0.84	0.011	5.6
Inner Housing	1.1	0.014	7.3
Planet Shaft	0.49	0.0064	3.3
Inner Carrier	2.7	0.035	17.9
Planet Gear	1.1	0.015	7.6
Sun Gear	0.55	0.0072	3.7
Ring Gear	4.6	0.059	30.6
Total	15	0.19	100

Figure 83: CO_2 Emission of the Manufacture and Transport Lifecycle Phase of the design

Use:

Summary

Mobile mode

Fuel and mobility type	Electric - family car
Country of use	World
Product mass (kg)	15
Distance (km per day)	30
Usage (days per year)	20
Product life (years)	1

Relative contribution of static and mobile modes

Mode	CO2 footprint (kg)	%
Static	0	
Mobile	0.2	100.0
Total	**0.2**	**100**

Breakdown of mobile mode by components

Component	CO2 footprint (kg)	%
Output Carrier	0.032	16.2
Outer Housing	0.015	7.8
Input Shaft	0.011	5.6
Inner Housing	0.015	7.3
Planet Shaft	0.0066	3.3
Inner Carrier	0.036	17.9
Planet Gear	0.015	7.6
Sun Gear	0.0074	3.7
Ring Gear	0.061	30.6
Total	**0.2**	**100**

Figure 84: CO_2 Emission of the Use Lifecycle Phase of the design

Summary

Disposal:

Component	End of life option	% recovered	CO2 footprint (kg)	%
Output Carrier	Reuse	100.0	0.034	8.5
Outer Housing	Recycle	100.0	0.057	14.3
Input Shaft	Reuse	100.0	0.012	2.9
Inner Housing	Recycle	100.0	0.053	13.4
Planet Shaft	Recycle	100.0	0.024	6.0
Inner Carrier	Recycle	100.0	0.13	32.9
Planet Gear	Reuse	100.0	0.016	4.0
Sun Gear	Reuse	100.0	0.0077	1.9
Ring Gear	Reuse	100.0	0.064	16.0
Total			0.4	100

EoL potential:

Component	End of life option	% recovered	CO2 footprint (kg)	%
Output Carrier	Reuse	100.0	-5.7	11.1
Outer Housing	Recycle	100.0	-12	23.7
Input Shaft	Reuse	100.0	-2	3.8
Inner Housing	Recycle	100.0	-12	22.2
Planet Shaft	Recycle	100.0	-0.84	1.6
Inner Carrier	Recycle	100.0	-4.6	8.8
Planet Gear	Reuse	100.0	-2.7	5.2
Sun Gear	Reuse	100.0	-1.3	2.5
Ring Gear	Reuse	100.0	-11	20.9
Total			-52	100

Figure 85: CO_2 Emission of the Disposal and End Of Life Phase of the design

G Part List

H Manufacturing Drawings

H.1 Input Shaft

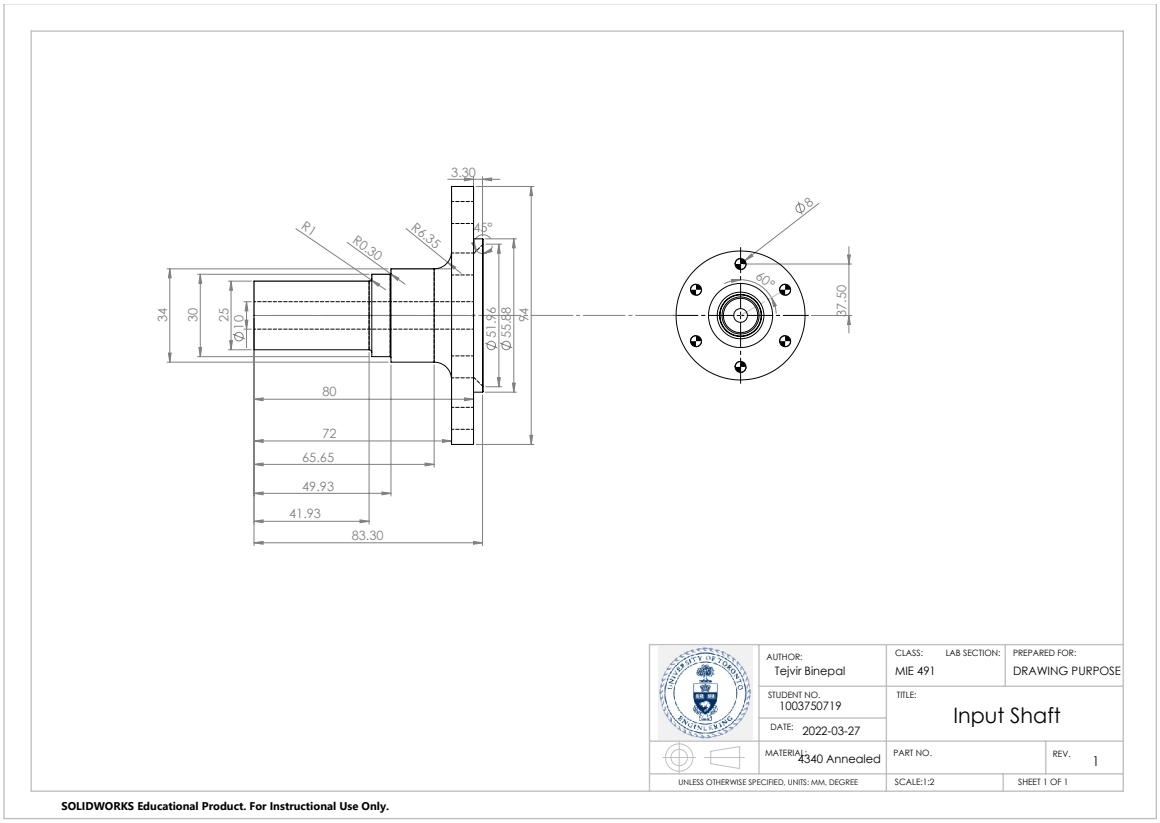

H.2 Planet Shaft

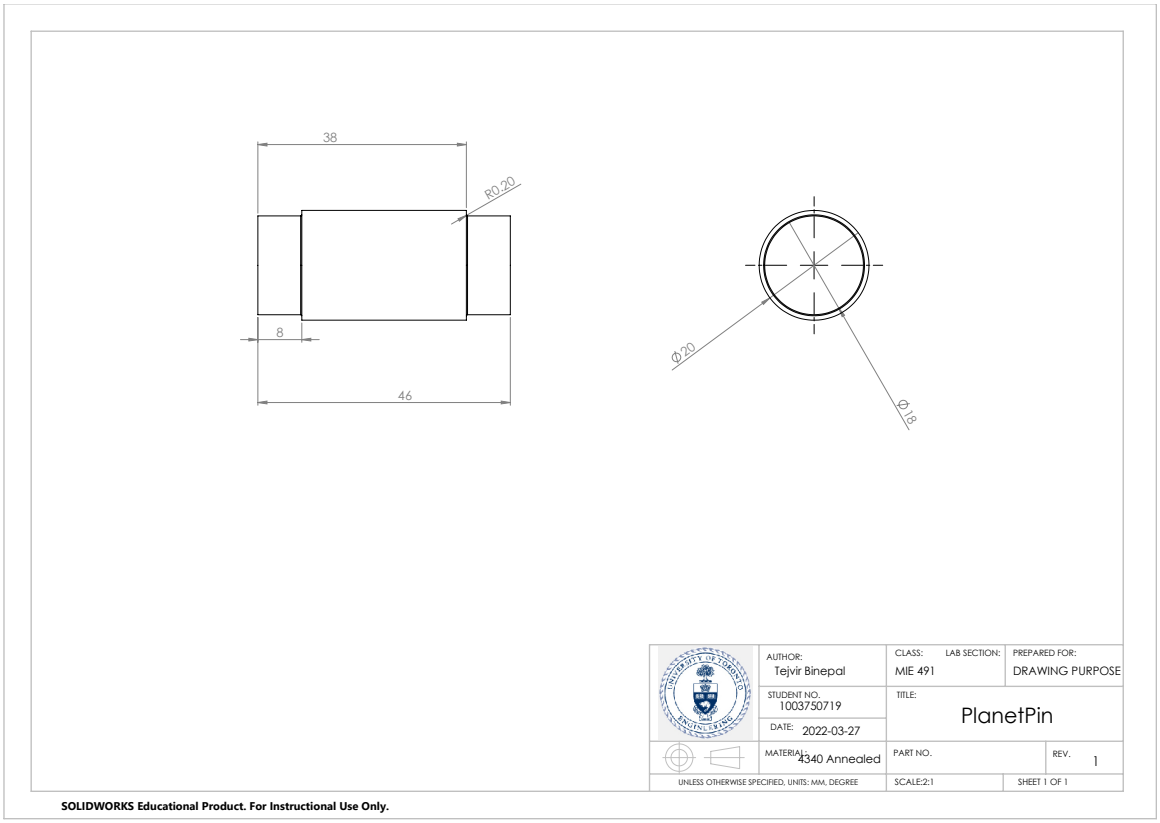

H.3 Output Carrier

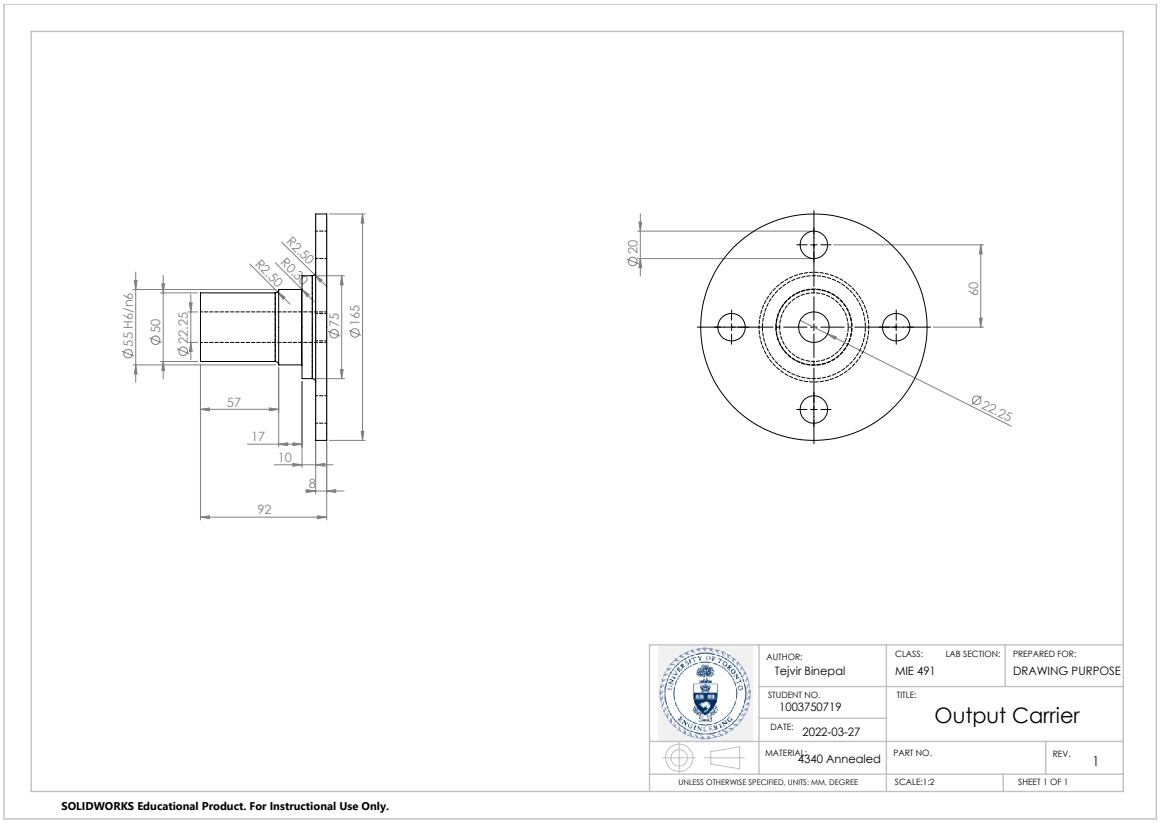

H.4 Input Carrier

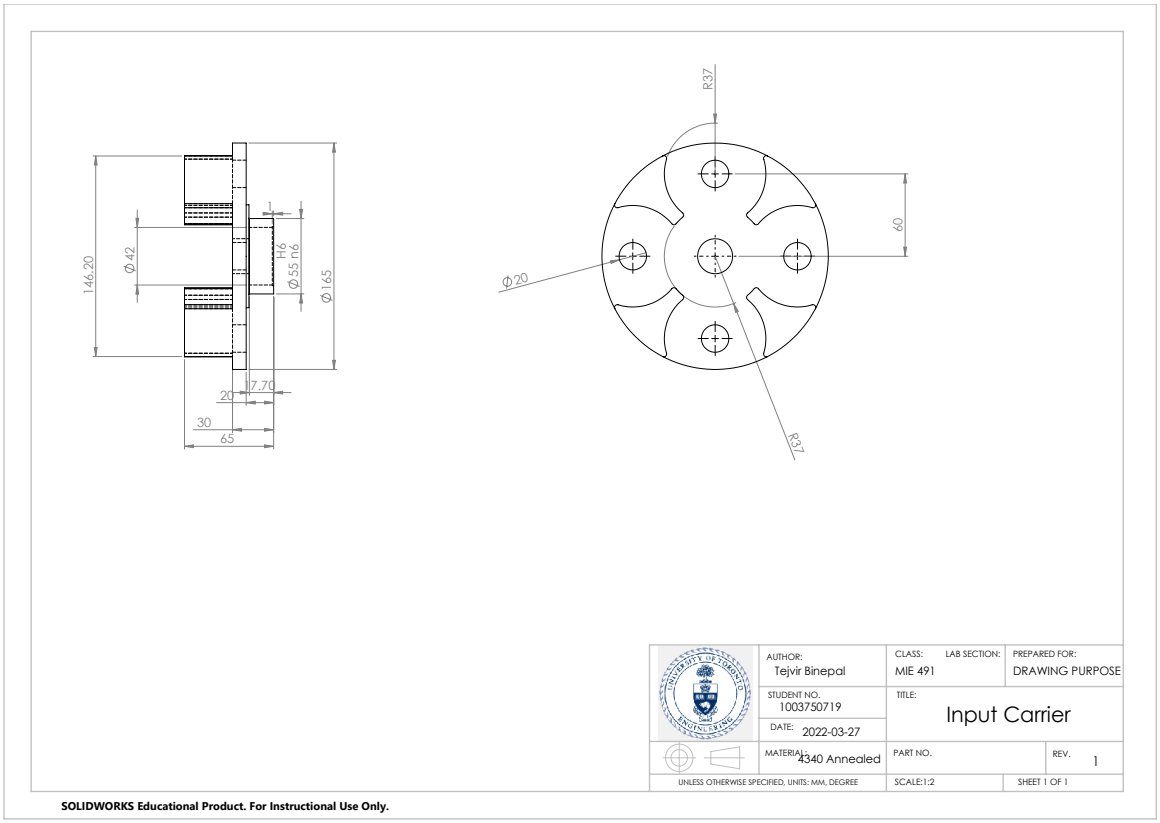

H.5 Ring Gear

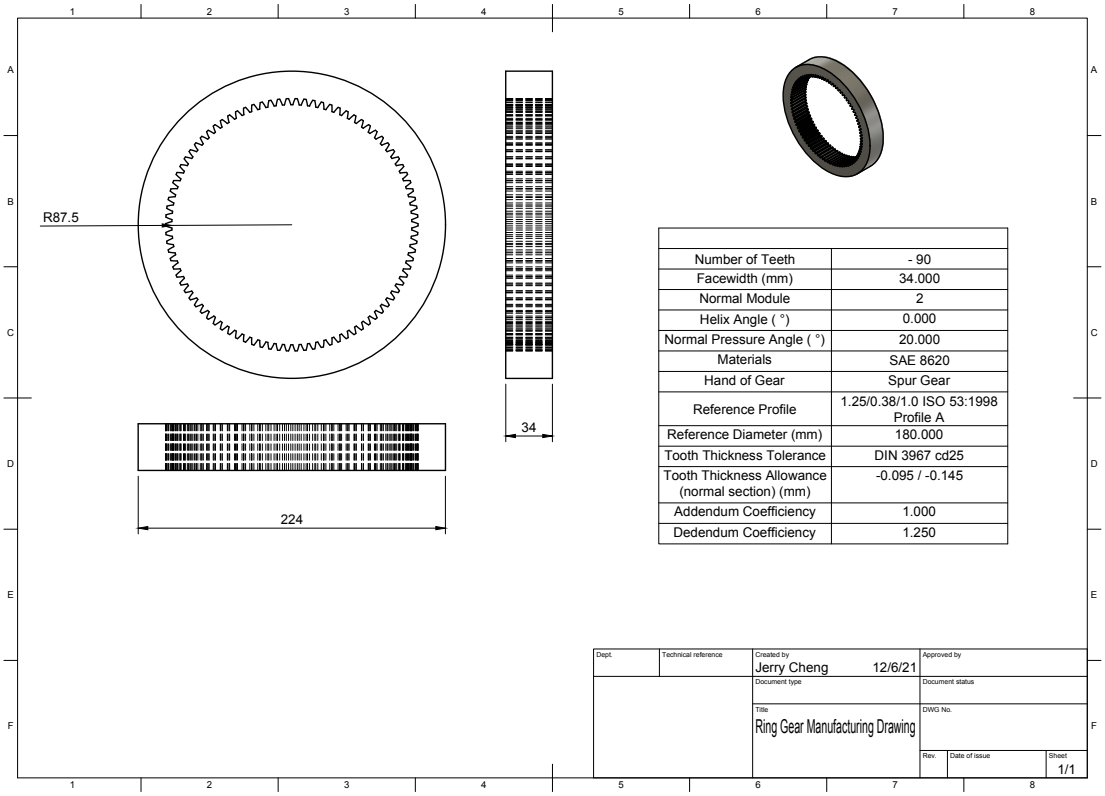

Number of Teeth	- 90
Facewidth (mm)	34.000
Normal Module	2
Helix Angle (°)	0.000
Normal Pressure Angle (°)	20.000
Materials	SAE 8620
Hand of Gear	Spur Gear
Reference Profile	1.25/0.38/1.0 ISO 53:1998 Profile A
Reference Diameter (mm)	180.000
Tooth Thickness Tolerance	DIN 3967 cd25
Tooth Thickness Allowance (normal section) (mm)	-0.095 / -0.145
Addendum Coefficiency	1.000
Dedendum Coefficiency	1.250

Dept.	Technical reference	Created by: Jerry Cheng 12/6/21	Approved by
		Document type	Document status
		Title: Ring Gear Manufacturing Drawing	DWG No.
			Rev. / Date of issue / Sheet: 1/1

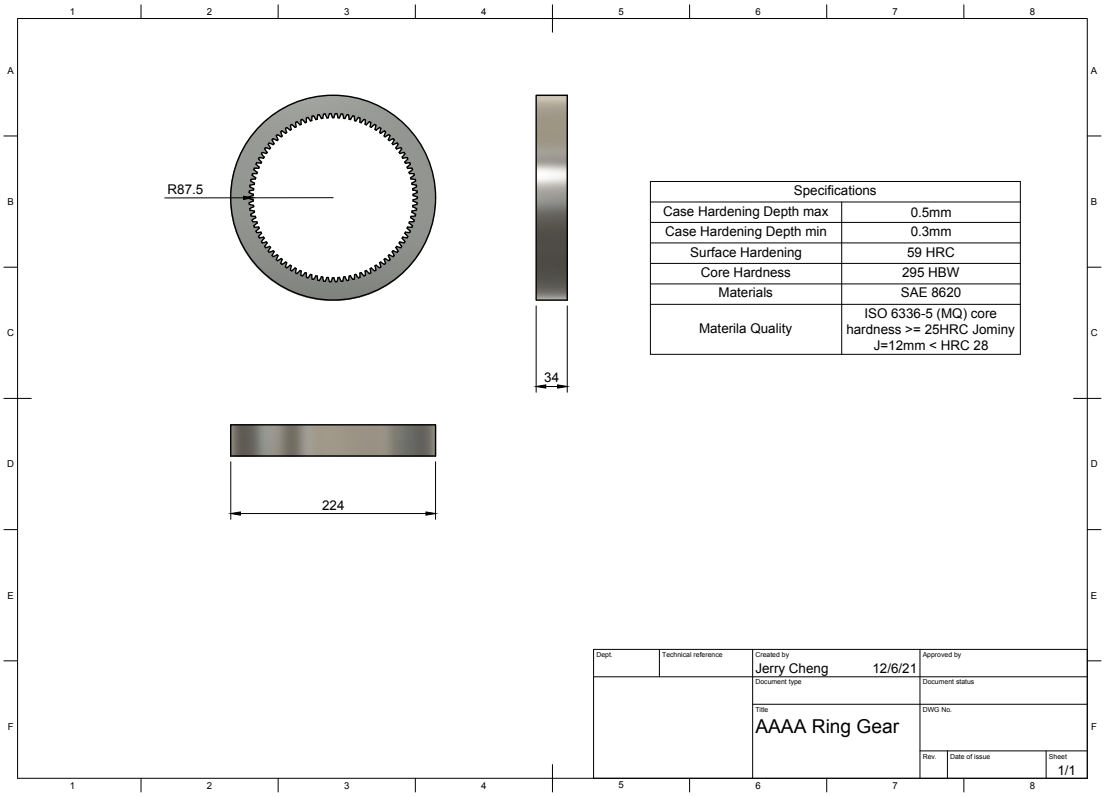

Specifications	
Case Hardening Depth max	0.5mm
Case Hardening Depth min	0.3mm
Surface Hardening	59 HRC
Core Hardness	295 HBW
Materials	SAE 8620
Materila Quality	ISO 6336-5 (MQ) core hardness >= 25HRC Jominy J=12mm < HRC 28

Dept.	Technical reference	Created by: Jerry Cheng 12/6/21	Approved by
		Document type	Document status
		Title: AAAA Ring Gear	DWG No.
			Rev. / Date of issue / Sheet: 1/1

H.6 Sun Gear

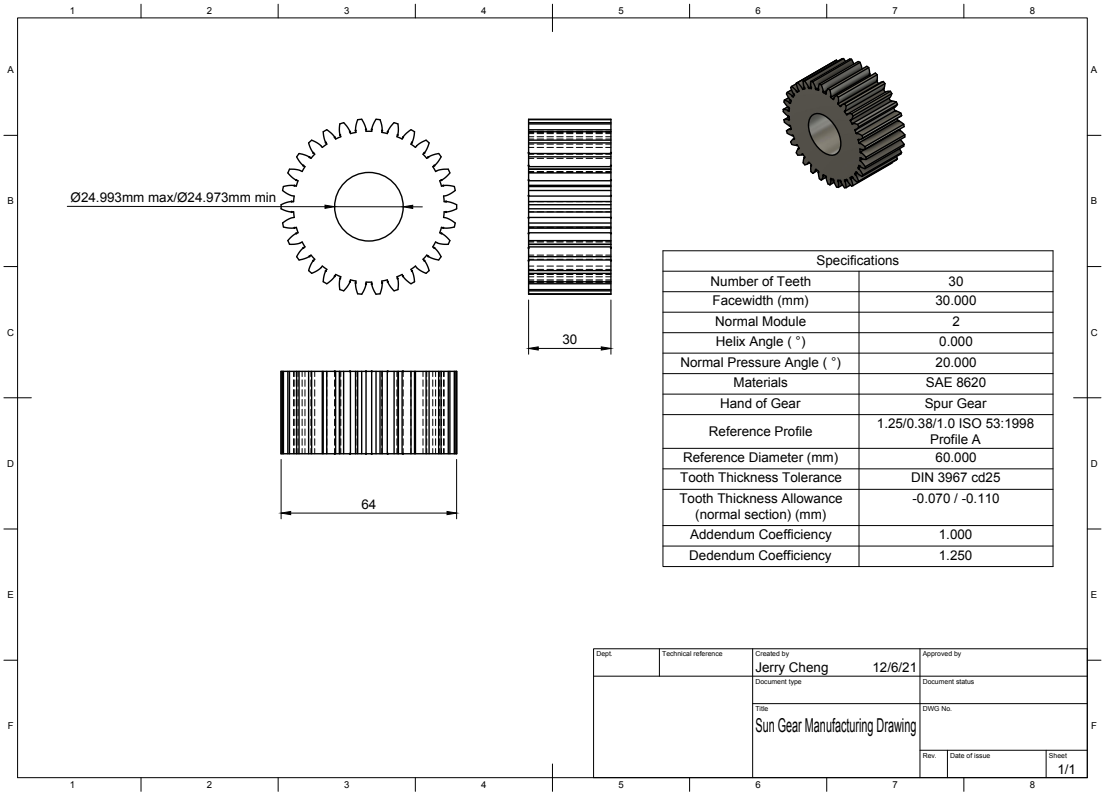

Specifications	
Number of Teeth	30
Facewidth (mm)	30.000
Normal Module	2
Helix Angle (°)	0.000
Normal Pressure Angle (°)	20.000
Materials	SAE 8620
Hand of Gear	Spur Gear
Reference Profile	1.25/0.38/1.0 ISO 53:1998 Profile A
Reference Diameter (mm)	60.000
Tooth Thickness Tolerance	DIN 3967 cd25
Tooth Thickness Allowance (normal section) (mm)	-0.070 / -0.110
Addendum Coefficiency	1.000
Dedendum Coefficiency	1.250

Dept.	Technical reference	Created by	Approved by
		Jerry Cheng 12/6/21	
		Document type	Document status
		Title: Sun Gear Manufacturing Drawing	DWG No.
			Rev. / Date of issue / Sheet: 1/1

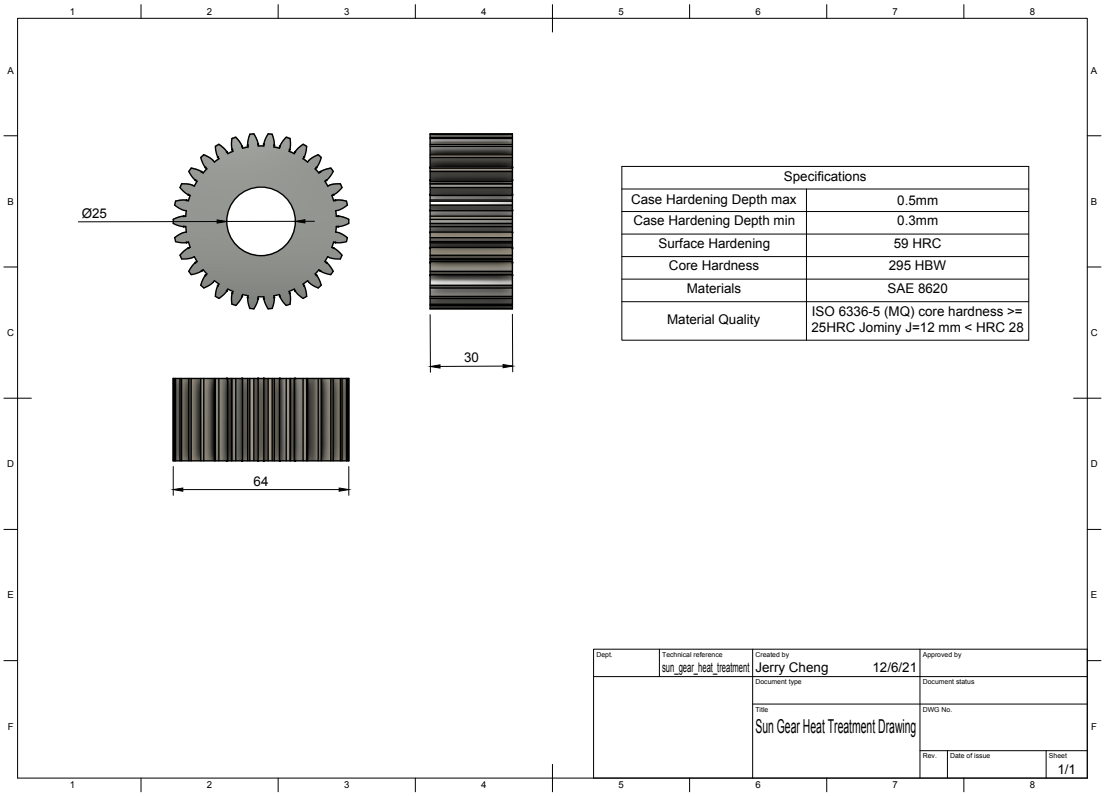

Specifications	
Case Hardening Depth max	0.5mm
Case Hardening Depth min	0.3mm
Surface Hardening	59 HRC
Core Hardness	295 HBW
Materials	SAE 8620
Material Quality	ISO 6336-5 (MQ) core hardness >= 25HRC Jominy J=12 mm < HRC 28

Dept.	Technical reference	Created by	Approved by
	sun_gear_heat_treatment	Jerry Cheng 12/6/21	
		Document type	Document status
		Title: Sun Gear Heat Treatment Drawing	DWG No.
			Rev. / Date of issue / Sheet: 1/1

H.7 Planet Gear

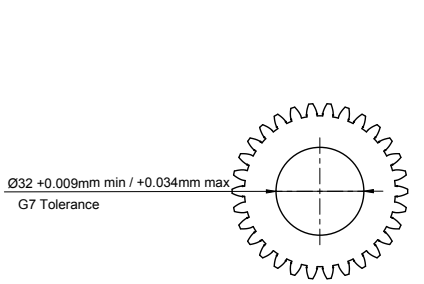

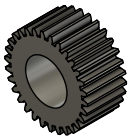

Specifications	
Number of Teeth	30
Facewidth (mm)	30.000
Normal Module	2
Helix Angle (°)	0.000
Normal Pressure Angle (°)	20.000
Materials	SAE 8620
Hand of Gear	Spur Gear
Reference Profile	1.25/0.38/1.0 ISO 53:1998 Profile A
Reference Diameter (mm)	60.000
Tooth Thickness Tolerance	DIN 3967 cd25
Tooth Thickness Allowance (normal section) (mm)	-0.070/-0.110
Addendum Coefficiency	1.000
Dedendum Coefficiency	1.250

Dept.	Technical reference	Created by	Approved by
		Jerry Cheng 12/5/21	
		Document type	Document status
		Title: Planet Gear Manufacturing Drawing	DWG No.
			Rev. / Date of issue / Sheet: 1/1

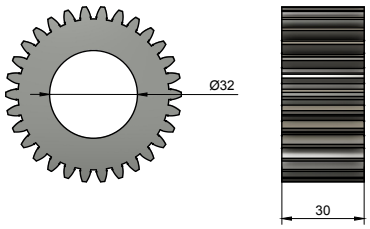

Specifications	
Case Hardening Depth max	0.5mm
Case Hardening Depth min	0.3mm
Surface Hardening	59 HRC
Core Hardness	295 HBW
Materials	SAE 8620
Material Quality	ISO 6336-5 (MQ) core hardness >= 25HRC Jominy J=12 mm < HRC 28

Dept.	Technical reference	Created by	Approved by
		Jerry Cheng 12/5/21	
		Document type	Document status
		Title: Planet Gear Heat Treatment Drawing	DWG No.
			Rev. / Date of issue / Sheet: 1/1

H.8 Assembly Instructions

Once all the components are ready, the gearbox would be assembly following the steps listed below:

Step 1
To start the full assembly, start with the four planet gears. First press fit the two bearings into the planet gear on each side. Then push the planet shaft though the two fitted bearings. The shoulder of the shaft should align with the two bearing's face when pressed in as shown in the diagram. Do the same thing for the four planet gears.

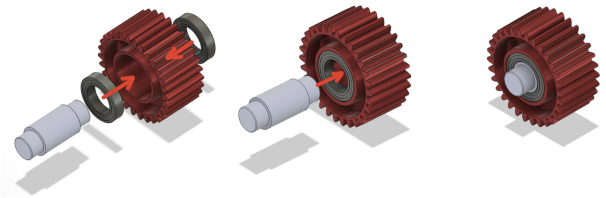

Figure 86: Assembly Process Step 1: Planet Gear Assembly

Step 2
Push the two Housing Bearings onto the input and output carriers respectively. Once press fit in place, the inner part of the bearing should be in contact with the carrier's built in spacer, while the bearing's face should also align with the carrier's shoulders.

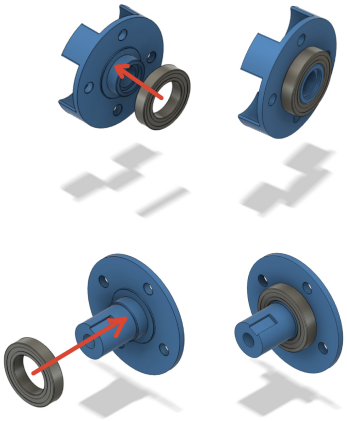

Figure 87: Assembly Process Step 2: Carrier Piece Assembly

Step 3
Place the Oil Seals in both Inner and Outer Housing. Be aware, the flat side of the oil seal should face outwards. Once in place, the oil seal should align perfectly within the indents inside the housings. Finally, place the two O-rings into the indents around the housing's edges. The placed O-rings should be slightly taller than the indents for future sealings.

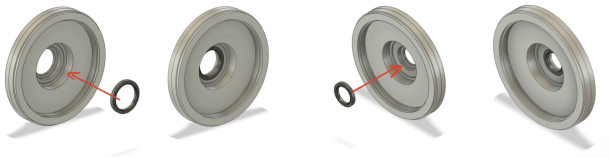

Figure 88: Assembly Process Step 3: Housing Assembly

Step 4
Next step is to assembly the carrier unit. First, press fit the pre-assembled planet gears from Step 1 into the Output Carrier. When press fitting, all the planet shafts should be in parallel to the output carrier's shaft. Then similarly, press fit the input carrier piece into the four planet shafts too.

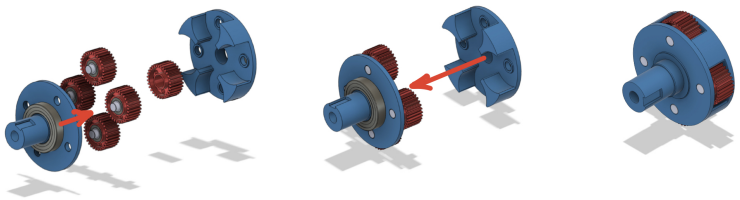

Figure 89: Assembly Process Step 4: Carrier Unit Assembly

The finished piece should have the two carriers contacting each other, while leaving 2mm of space between the planet gears and the input and output carrier respectively. The top view of the piece is shown below illustration the placement.

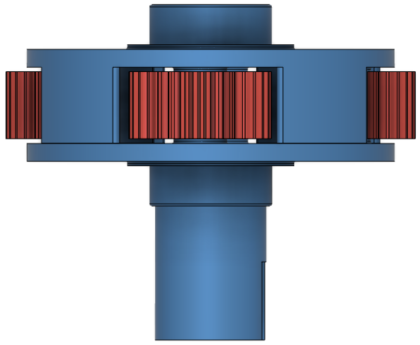

Figure 90: Top View of Carrier Assembled Pieces' Spacing

Step 5
This step requires to bring all the pieces together. First fit the ring gear through the assembled carrier unit from step 4. Next, press fit the two housings onto the carriers. The housing bearings from step 2 should be tightly connected with the indents inside the two housing pieces.

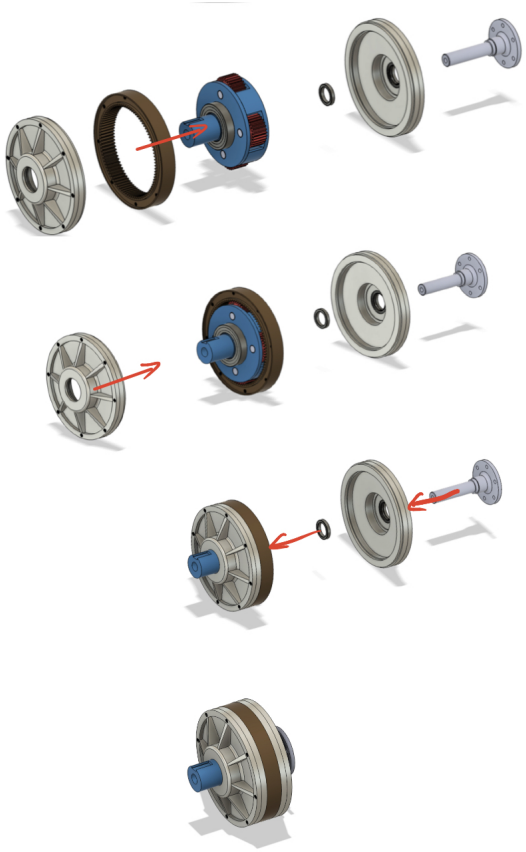

Figure 91: Energy and CO_2 Summary of the design

Then press fit the carrier bearing into the deep groove of the input carrier (As shown in the diagram below). Finally, similar to the outer housing, press fit the inner housing into the housing bearing from step 2. Lastly, the input shaft will be pushed all the way through the gearbox. This step is the most crucial part since it needs to go through both the carrier bearing and the sun gear. In addition, any misalignment between the input and output shaft should be eliminated in this step.

Step 6
Push the 8 M7 screws through the entire gearbox and bolt them in place. Make sure there are at least 5 threads remain on the other end after the nuts are threaded in place. This is essential as FSAE guidline stated this requirement as the safety guideline.

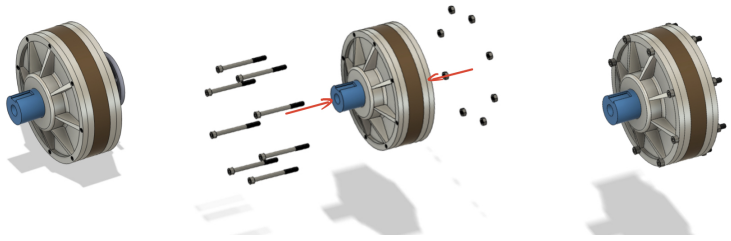

Figure 92: Energy and CO_2 Summary of the design

Step 7
Finally, before press fitting the input shaft into the gearbox, place the six M8 screws into the screw

holes on the input shaft first. Press fit the input shaft through the carrier bearing and the sun gear. Once in place, the input shaft's shoulder should be perfectly align with the inner housing and the oil seal. Lastly, screw the six screws onto the motor itself and finish the assembly.

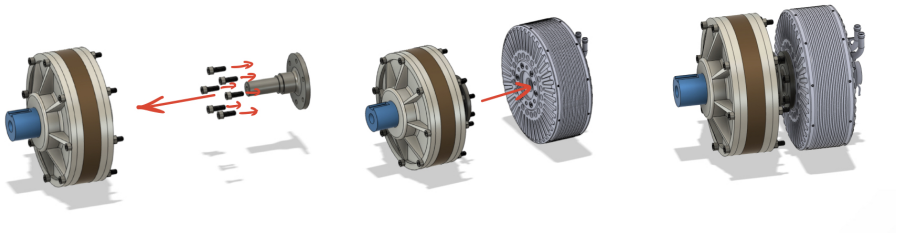

Figure 93: Energy and CO_2 Summary of the design

I Testing Plans

I.1 Dyno Testing and Cooling Testing

Objective: A chassis eddy current dyno can be used to determine the performance of the gearbox & drive train when integrated in the car. The measured performance from the chassis dyno can be used to determine the actual efficiency of the design by comparing it to the curve shown in Figure 94. The dyno testing can be also used to validate whether the cooling system provides enough cooling during all RPM ranges by monitoring the temperature of the lubricant during the run
Requirements: The dyno testing requires a race ready car, access to a chassis dyno machine, data-acquisition system and sensors connected to the rollers. To validate performance of the cooling system, one temperature RTD sensor is required to monitor the lubricant inside the gearbox. Two T-Type Thermocouples attached to a T-fitting with hose barb ends attached on either side to connect to the loop. A handheld anemometer to measure air properties (Velocity and Temperature).Three team members and a driver should be present during the testing.
Procedure:

1. Start by mounting the car on the chassis dyno and securing it with straps. Ideally the accumulator (Battery Pack) should be off the car and the motor should be powered by an external high voltage supply

2. Fill up the prescribed gearbox with SAE 140 Oil and the high power electronics cooling system with distilled water.

3. Turn on the vehicle when the electrical safety officer deems it safe to do so. Begin by slowly accelerating and ensuring the rollers are rotating and sending the data to the software. The rollers might have to be bump started if there is not enough power from the car

4. Hold a constant RPM and then gradually increase the RPM making sure to hold different RPM's to match with the processing frequency of the data acquisition system.

5. A team member should be recording the air velocity and temperature behind the oilbox radiator using the handheld anemometer

6. A team member should be monitoring the temperature of the lubricant in the gearbox making sure it stays below 40 +/- error of the thermocouple error.

7. Make sure the temperature of the motor and inverter stay below the acceptable thermal safety limits. After ensuring all RPM ranges have been recorded, slowly decreasing speed. Make sure the car wheels and roller come to complete stop. Save the data, turn off all sensors.

8. Make sure the high power tractive system is turned off and it is safe to exit the vehicle
9. Save the recorded results and turn off Repeat three runs of the same procedure, spaced across multiple days to ensure consistency in test results

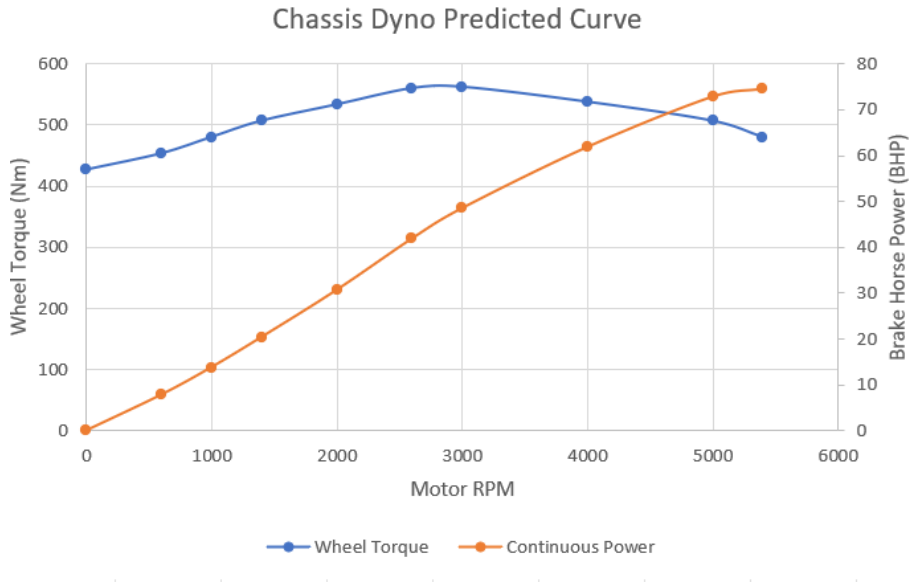

Figure 94: Predicted Performance with a 0.91 efficiency

J Modal Analysis Results on Other Components

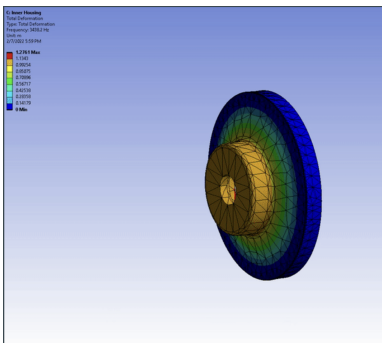

Mode	Frequency(Hz)
1	3438.2
2	4655.2
3	4667.3
4	7911.6
5	7921.4

Figure 95: Modal Analysis on Ansys for Inner Housing

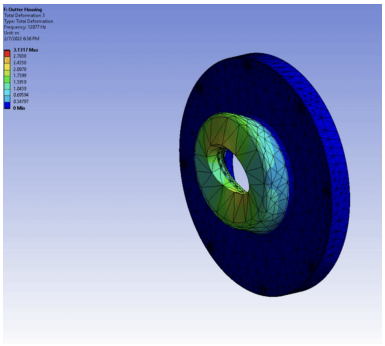

Mode	Frequency(Hz)
1	3054.2
2	3077.1
3	3708.6
4	7657.9
5	8681.3

Figure 96: Modal Analysis on Ansys for Outer Housing

K System Torsional Vibration:

Torsional vibration is caused when the torsional shear stress is transmitted from input shaft to output shaft. When the motor is subjecting an external moment to the input and output shaft, due to the polar moment of inertia and the spring effect of the material, the shafts have a tendency to behave like a spring-mass system, causing the system to undergo torsional vibration.

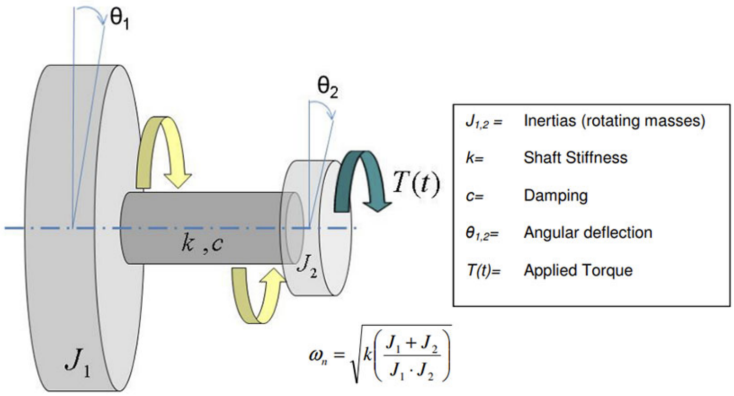

Figure 97: Simplified Torsional Vibration Model [**?**]

In the final design, the torsional vibration model can be derived from the carriers and the input shaft as shown below:

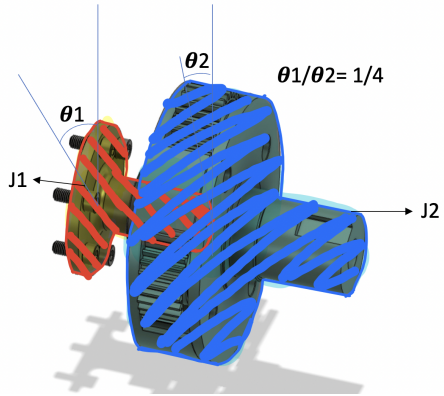

Figure 98: Similar Torsional Vibration Model Developed for Our Final Design [**?**]

$$T = \frac{1}{2}J_1\dot{\theta_1}^2 + \frac{1}{2}J_2\dot{\theta_2}^2 = \frac{1}{2}J_1\dot{\theta_1}^2 + \frac{1}{2}J_2(\dot{\frac{n_1}{n_2}\theta_1})^2 \tag{28}$$

The equivalent spring coefficient of a torsional system can be found using the equation below[32]:

$$k_i = \frac{GI_i}{l_i} \tag{29}$$

$$(J_1 + J_2(\frac{n_1}{n_2})^2)\ddot{\theta_1} + k_i\theta_1 = M(t) \tag{30}$$

Based on this equation, the natural frequency of the torsional vibration for the shaft can be estimated as:

$$w_n = \sqrt{\frac{k_{eq}}{J_{eq}}} \tag{31}$$

where $k_{eq} = k_i$ and $J_{eq} = (J_1 + J_2(\frac{n_1}{n_2})^2)$

$G = 77 \times 10^9 Pa$ is taken as the shear modulus for carbon steel used in the shaft; $\frac{n_1}{n_2} = 1/4$ based on the total gear ratio, and the input shaft length is measured as 9cm. Finally plug in the values from the table below, the final system torsional natural frequency is calculated to be around 550Hz.

Table 29: Mass and Polar Moment of Inertia around the Rotational Axis for Each Moving Components

	m(g)	**J** $(kg * m^2)$
Sun Gear	294.363	1.774*10^8
Planet Gear	284.713	1.791*10^8
Output Carrier	2398.269	4.889*10^9
Input Carrier	2677.312	9.99*10^9
Input Shaft	819.817	5.164*10^8

It can be concluded that the lowest natural frequency for the input shaft is 3014.2 Hz and for the output shaft is 2354.3 Hz. When the external frequency subjected on the gearbox is around this frequency, it will cause the system to resonate and will eventually lead to failure. Therefore, the forced vibration frequency range should be ideally lower than those values.

L Source Code for Vibration Analysis

```
fs = 20E3;              % Sample Rate (Hz)

Np = 30;                % Number of teeth on pinion
Ng = 30;                % Number of teeth on gear

fPin = 55;           % Pinion (Input) shaft frequency (Hz)

fGear = fPin*Np/Ng; % Gear (Output) shaft frequency (Hz)

fMesh = fPin*Np;      % Gear Mesh frequency (Hz)

t = 0:1/fs:20-1/fs;

vfIn = 0.4*sin(2*pi*fPin*t);      % Pinion waveform
vfOut = 0.2*sin(2*pi*fGear*t);    % Gear waveform

vMesh = sin(2*pi*fMesh*t);        % Gear-mesh waveform
vTotal = vfIn + vfOut + vMesh;
```

```
[minSignal, indexOfMin] = min(vTotal);
[maxSignal, indexOfMax] = max(vTotal);

tMin = t(indexOfMin);
tMax = t(indexOfMax);

vMin = 0.4*sin(2*pi*fPin*tMin) + 0.2*sin(2*pi*fGear*tMin) + sin(2*pi*fMesh*tMin);
vMax = 0.4*sin(2*pi*fPin*tMax) + 0.2*sin(2*pi*fGear*tMax) + sin(2*pi*fMesh*tMax);

xline(tMax, 'Color', 'r', 'LineWidth', 2);
xline(tMin, 'Color', 'r', 'LineWidth', 2);

% textLabel = sprintf(' Max of %.2f at t=%f', maxSignal, tMax);
% text(tMax, maxSignal, textLabel, 'fontSize', 15, 'Color', 'r', 'VerticalAlignment','bottom')
% ylim([-1.2, 1.2])

plot(t, vTotal)
xlim([0 0.25])
xlabel('Time (s)')
ylabel('Amplitude (mm)')


ipf = fGear;
fImpact = 2000;

tImpact = 0:1/fs:2.5e-4-1/fs;
xImpact = sin(2*pi*fImpact*tImpact)/3;

xComb = zeros(size(t));

Ind = (0.25*fs/fMesh):(fs/ipf):length(t);
Ind = round(Ind);
xComb(Ind) = 1;

xPer = 2*conv(xComb,xImpact,'same');

vNoFault = vfIn + vfOut + vMesh;
vFault = vNoFault + xPer;

vNoFaultNoisy = vNoFault + randn(size(t))/5;
vFaultNoisy = vFault + randn(size(t))/5;

subplot(2,1,1)
plot(t,vNoFaultNoisy)
xlabel('Time (s)')
ylabel('Amplitude (mm)')
xlim([0.0 0.3])
ylim([-2.5 2.5])
title('Noisy Signal for Healthy Gear')


subplot(2,1,2)
plot(t,vFaultNoisy)
xlabel('Time (s)')
ylabel('Amplitude (mm)')
xlim([0.0 0.3])
ylim([-2.5 2.5])
title('Noisy Signal for Faulty Gear')
hold on
MarkX = t(Ind(1:3));
MarkY = 2.5;
plot(MarkX,MarkY,'rv','MarkerFaceColor','red')
hold off

[Spect,f] = pspectrum([vFaultNoisy' vNoFaultNoisy'],fs,'FrequencyResolution',0.2,'FrequencyLimits',[0 500]);

figure
plot(f,10*log10(Spect(:,1)),f,10*log10(Spect(:,2)),':')
xlabel('Frequency (Hz)')
ylabel('Power Spectrum (dB)')

hold on
plot(fGear,0,'rv','MarkerFaceColor','red')
plot(fPin,0,'gv','MarkerFaceColor','green')
plot(fMesh,0,'bv','MarkerFaceColor','blue')
hold off

legend('Faulty','Healthy','f_{Gear}','f_{Pinion}','f_{Mesh}')
```